

See discussions, stats, and author profiles for this publication at: <https://www.researchgate.net/publication/41506880>

Lipid Peroxyl Radicals Mediate Tyrosine Dimerization and Nitration in Membranes

ARTICLE *in* CHEMICAL RESEARCH IN TOXICOLOGY · FEBRUARY 2010

Impact Factor: 3.53 · DOI: 10.1021/tx900446r · Source: PubMed

CITATIONS

39

READS

57

7 AUTHORS, INCLUDING:



[Silvina Bartesaghi](#)

University of the Republic, Uruguay

22 PUBLICATIONS 463 CITATIONS

[SEE PROFILE](#)



[Madia Trujillo](#)

University of the Republic, Uruguay

56 PUBLICATIONS 3,036 CITATIONS

[SEE PROFILE](#)



[Marcos Lopez](#)

Fundación Cardiovascular de Colombia

25 PUBLICATIONS 854 CITATIONS

[SEE PROFILE](#)



[Rafael Radi](#)

University of the Republic, Uruguay

308 PUBLICATIONS 22,609 CITATIONS

[SEE PROFILE](#)



NIH Public Access

Author Manuscript

Chem Res Toxicol. Author manuscript; available in PMC 2012 November 26.

Published in final edited form as:

Chem Res Toxicol. 2010 April 19; 23(4): 821–835. doi:10.1021/tx900446r.

Lipid peroxyl radicals mediate tyrosine dimerization and nitration in membranes

Silvina Bartesaghi,

Departamento de Histología y Embriología, Facultad de Medicina, Universidad de la República, Uruguay. Phone: +598-2-9249561, Fax: +598-2-9249563

Departamento de Bioquímica, Facultad de Medicina, Universidad de la República, Uruguay. Phone: +598-2-9249561, Fax: +598-2-9249563

Center for Free Radical and Biomedical Research, Facultad de Medicina, Universidad de la República, Uruguay. Phone: +598-2-9249561, Fax: +598-2-9249563

Jorge Wenzel,

Departamento de Bioquímica, Facultad de Medicina, Universidad de la República, Uruguay. Phone: +598-2-9249561, Fax: +598-2-9249563

Center for Free Radical and Biomedical Research, Facultad de Medicina, Universidad de la República, Uruguay. Phone: +598-2-9249561, Fax: +598-2-9249563

Madia Trujillo,

Departamento de Bioquímica, Facultad de Medicina, Universidad de la República, Uruguay. Phone: +598-2-9249561, Fax: +598-2-9249563

Center for Free Radical and Biomedical Research, Facultad de Medicina, Universidad de la República, Uruguay. Phone: +598-2-9249561, Fax: +598-2-9249563

Marcos López,

Department of Biophysics and Free Radical Research Center, Medical College of Wisconsin, Milwaukee WI 53226, USA. Phone: + 414-456-4000, Fax: +414-456-6512

Joy Joseph,

Department of Biophysics and Free Radical Research Center, Medical College of Wisconsin, Milwaukee WI 53226, USA. Phone: + 414-456-4000, Fax: +414-456-6512

Balaraman Kalyanaraman, and

Department of Biophysics and Free Radical Research Center, Medical College of Wisconsin, Milwaukee WI 53226, USA. Phone: + 414-456-4000, Fax: +414-456-6512

Rafael Radi

Departamento de Bioquímica, Facultad de Medicina, Universidad de la República, Uruguay

Center for Free Radical and Biomedical Research, Facultad de Medicina, Universidad de la República, Uruguay

Silvina Bartesaghi: sbartesa@fmed.edu.uy; Jorge Wenzel: jwenzel@fmed.edu.uy; Madia Trujillo: madiat@fmed.edu.uy; Marcos López: marcoslopez@mcw.edu; Joy Joseph: jjoseph@mcw.edu; Balaraman Kalyanaraman: balarama@mcw.edu

Abstract

*To whom correspondence should be addressed: Dr Rafael Radi, Departamento de Bioquímica, Facultad de Medicina, Avda. General Flores 2125, 11800 Montevideo, Uruguay. Phone: +598-2-9249561, Fax: +598-2-9249563, rradi@fmed.edu.uy.

Protein tyrosine dimerization and nitration by biologically-relevant oxidants usually depend on the intermediate formation of tyrosyl radical ($\cdot\text{Tyr}$). In the case of tyrosine oxidation in proteins associated to hydrophobic compartments, the participation of unsaturated fatty acids in the process must be considered since they typically constitute preferential targets for the initial oxidative attack. Thus, we postulate that lipid-derived radicals mediate the one-electron oxidation of tyrosine to $\cdot\text{Tyr}$, which can afterwards react with another $\cdot\text{Tyr}$ or with nitrogen dioxide ($\cdot\text{NO}_2$) to yield 3,3'-dityrosine or 3-nitrotyrosine within the hydrophobic structure, respectively. To test this hypothesis, we have studied tyrosine oxidation in saturated and unsaturated fatty acid-containing phosphatidylcholine (PC) liposomes with an incorporated hydrophobic tyrosine analog BTBE (*N-t*-BOC L-tyrosine *tert*-butyl ester) and its relationship with lipid peroxidation promoted by three oxidation systems, namely peroxy nitrite, hemin and 2,2'-azobis (2-amidinopropane) hydrochloride (ABAP). In all cases, significant tyrosine (BTBE) oxidation was seen in unsaturated PC liposomes, in a way that was largely decreased at low oxygen concentrations. Tyrosine oxidation levels paralleled those of lipid peroxidation (*i.e.* malondialdehyde and lipid hydroperoxides) and lipid-derived radicals and BTBE phenoxyl radicals were simultaneously detected by ESR-spin trapping, supporting an association between the two processes. Indeed, α -tocopherol, a known reactant with lipid peroxyl radicals (LOO^\bullet), inhibited both tyrosine oxidation and lipid peroxidation induced by all three oxidation systems. Moreover, oxidant-stimulated liposomal oxygen consumption was dose-dependently inhibited by BTBE but not by its phenylalanine analog, BPBE (*N-t*-BOC L-phenylalanine *tert*-butyl ester), providing a direct evidence for the reaction between LOO^\bullet and the phenol moiety in BTBE, with an estimated second order rate constant of $4.8 \times 10^3 \text{ M}^{-1}\text{s}^{-1}$. In summary, the data presented herein demonstrate that LOO^\bullet mediate tyrosine oxidation processes in hydrophobic compartments and provide a new mechanistic insight to understand protein oxidation and nitration in lipoproteins and biomembranes.

Introduction

Tyrosine dimerization and nitration to 3,3'-dityrosine and 3-nitrotyrosine (3-nitro-Tyr), respectively, represent biologically-relevant oxidative post-translational modifications in proteins generated by the reactions with reactive oxygen and nitrogen intermediates both *in vitro* and *in vivo*. These tyrosine oxidation processes depend on the intermediate formation of tyrosyl radical ($\cdot\text{Tyr}$), a transient species formed by the one-electron oxidation of tyrosine. For instance, 3,3'-dityrosine formation results from the termination reaction between two $\cdot\text{Tyr}$ radicals with the formation of a new C-C bond; 3,3'-dityrosine participates in protein cross-linking (1) and also serves as a marker for oxidatively damaged proteins. Indeed, elevated levels of 3,3'-dityrosine can be found as a product of aging, inflammation, exposure to UV and γ -radiation and other oxidative stress conditions (2–4). Tyrosine nitration in biological systems is also a free radical process (5) produced by nitric oxide ($\cdot\text{NO}$)-derived oxidants such as peroxy nitrite¹ and nitrogen dioxide radical ($\cdot\text{NO}_2$) (5); typically, the final step in nitration involves the diffusion-controlled reaction of $\cdot\text{Tyr}$ with $\cdot\text{NO}_2$. The product of this reaction, 3-nitro-Tyr, is a footprint of nitro-oxidative damage *in vivo*, being revealed as a strong biomarker and predictor of disease progression in conditions such as inflammation, cardiovascular disease and neurodegeneration (6–9). Protein tyrosine nitration could result in dramatic changes in protein structure and can affect biological activity either by a loss (*e.g.* Mn-SOD (10–12) or by a gain of function (*e.g.* nerve growth factor (13) and cytochrome c (14,15); recently reviewed in (16)). As 3,3'-dityrosine and 3-nitro-Tyr formation require the intermediacy of $\cdot\text{Tyr}$, both tyrosine oxidation products can be formed simultaneously in oxidizing environments where $\cdot\text{NO}$ and reactive oxygen

¹IUPAC recommended names for peroxy nitrite anion (ONOO^-) and peroxy nitrous acid (ONO_2) ($\text{pK}_{\text{a}} = 6.8$) are oxoperoxonitrate (1-) and hydrogen oxoperoxonitrate, respectively. The term peroxy nitrite is used to refer to the sum of ONOO^- and ONO_2 .

intermediate radicals (*e.g.* superoxide radical, $O_2^{\bullet-}$ hydrogen peroxide, H_2O_2) coexist. Specifically, this chemistry can be performed by peroxy nitrite, a powerful oxidant and cytotoxic species formed *in vivo* by the diffusion-controlled reaction between $\bullet NO$ and $O_2^{\bullet-}$ (5, 17, 19).

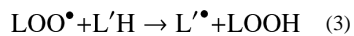
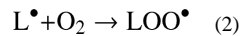
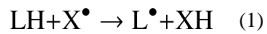
Peroxy nitrite does not directly react with tyrosine (20) but promotes tyrosine dimerization and nitration due to the reactions of peroxy nitrite-derived species such hydroxyl radical ($\bullet OH$), carbonate radical ($CO_3^{\bullet-}$), $\bullet NO_2$ or high oxidation state of redox-active metal centers ($Me^{(n+1)+} = O$, where Me is Fe, Cu or Mn) (recently reviewed in (21)) that can oxidize tyrosine to yield $\bullet Tyr$; which then combines with another $\bullet Tyr$ or $\bullet NO_2$ to yield 3,3'-dityrosine or 3-nitro-Tyr, respectively (22). For free tyrosine or tyrosine analogs in aqueous solution the 3,3'-dityrosine/3-nitro-Tyr ratio after peroxy nitrite exposure typically range in values of 1/20–1/25; however, this ratio may change if peroxy nitrite is added as a single bolus or by slow infusion and depends on the tyrosine and peroxy nitrite concentration and may become smaller in proteins, reflecting the relative ease of the nitration reaction respect to the dimerization reaction, due to diffusional and steric limitations. In addition, other tyrosine oxidation products from peroxy nitrite can be formed, including the hydroxylated derivative 3,4-dihydroxyphenylalanine (DOPA) (23). Of note, 3-nitro-Tyr was initially considered a specific marker of peroxy nitrite; however, there is now agreement that tyrosine nitration can also occur biologically by peroxy nitrite-independent mechanisms which include hydrogen peroxide (H_2O_2)-dependent nitrite oxidation catalyzed by heme (24) and hemoperoxidases (*e.g.* myeloperoxidase (25), eosinophil peroxidase (26), reviewed in (5)), pathways that also lead to the formation of 3,3'-dityrosine.

Protein tyrosine dimerization and nitration sites and yields depend on the protein structure, oxidation mechanism and the environment where the protein tyrosine residues are located (22, 27). In this last regard, most of the mechanistic studies of oxidation for free and protein tyrosines have been performed in aqueous solution (10, 11, 28). However, many protein tyrosine residues shown to be dimerized and nitrated either *in vitro* and *in vivo* are associated to non-polar compartments, such as red cell membrane proteins (29–31), mitochondrial membrane proteins (32–34), sarcoplasmic reticulum Ca^{2+} ATPase, microsomal glutathione S-transferase (35), apolipoproteins A and B (3, 25, 36). Within these proteins, in some cases oxidized tyrosines have been shown in cytosolic or extracellular domains (*e.g.* Tyr 192, apoA-I (36)), but in other cases in domains closely related to lipids (*e.g.* Tyr 39 in α -synuclein (37)). Also, reversible interactions of phospholipids with proteins can modulate tyrosine oxidation yields and sites, as observed for the cases of apoA-I (36) α -synuclein (38) and matrix metalloproteinase MMP-13 during wound repair (39).

Physico-chemical factors controlling tyrosine oxidation in hydrophobic biocompartments such as biomembranes and lipoproteins differ from those in aqueous solution. For example, hydrophobic phases contain a high concentration of unsaturated fatty acids and exclude key antioxidant molecules that are potent inhibitors of tyrosine oxidation in aqueous phases such as glutathione (22). In addition, there is a differential distribution of oxidizing species in the lipid *vs* aqueous phase: while $\bullet NO_2$ can readily diffuse, concentrate and react in the hydrophobic compartment (40), $CO_3^{\bullet-}$ and hemeproteins have limited action due to the restricted permeation and steric restrictions, respectively. Another important aspect to consider, is the restricted lateral diffusion of $\bullet Tyr$ in the organized structure of membranes which limits the dimerization process and results in smaller 3,3'-dityrosine/3-nitro-Tyr ratios than those observed in aqueous phases (~1/100–1/400) (41).

The need to further investigate tyrosine oxidation mechanisms in hydrophobic environments has led to the development of probes such as hydrophobic tyrosine analogs (41, 42) and tyrosine-containing transmembrane peptides (42). In this regard, *N-t*-BOC L-tyrosine *tert*

butyl ester (BTBE) is a stable tyrosine analog that we have previously used to study peroxy nitrite and MPO-mediated tyrosine oxidation in lipid phases including liposomes and biomembranes (41–43). BTBE can be efficiently incorporated (>98%) into phosphatidylcholine (PC) liposomes and the formation of BTBE-derived phenoxy radicals and oxidation products (*i.e.* 3-nitro-BTBE, 3,3'-di-BTBE and 3-hydroxy-BTBE) evaluated (41–43). Previous observations (41, 43) and kinetic considerations prompted us to investigate in depth how the unsaturated fatty acids present in high concentration in membranes and other hydrophobic compartments may influence peroxy nitrite-mediated tyrosine oxidation mechanisms and yields. Indeed, peroxy nitrite is a known inductor of lipid peroxidation *via* free radical reactions (44) initiated after the homolysis of ONOOH to •OH and •NO₂ (21); unsaturated fatty acids readily react with •OH ($k = 1 \times 10^{10} \text{ M}^{-1}\text{s}^{-1}$) (45) and to a lesser extent with •NO₂ ($k = 2 \times 10^5 \text{ M}^{-1}\text{s}^{-1}$ for linoleate at pH 9.4) (46, 47), both of which promote hydrogen abstraction from a *bis*-allylic hydrogen to initiate a chain reaction. Therefore, at a first glance an increased level of unsaturation in phosphatidylcholine (PC) liposomes could result on a decrease of tyrosine oxidation yields. However, peroxy nitrite-dependent BTBE nitration and dimerization yields were still high in PC liposomes containing a large polyunsaturated fatty acid content (41). These data indicate that a simple competition kinetic model does not apply and suggest that lipid-derived radicals mediate tyrosine oxidation within the membrane. Indeed, lipid peroxidation is an oxygen-dependent process that results in the formation of peroxy (LOO[•]) (Eqs. 1–3), and secondarily, alkoxyl radicals (LO[•]) (48–50).



These lipid-derived radicals are reactive species that can in turn oxidize biological targets (RH) including protein side chains (51). According to the one-electron redox potential of alkoxyl ($E^\circ \text{ LO}^\bullet/\text{LOH} = 1.76 \text{ V}$) and peroxy radicals ($E^\circ \text{ LOO}^\bullet/\text{LOOH} = 1.02 \text{ V}$), is thermodynamically possible for both species to oxidize tyrosine to the phenoxy radical ($E^\circ \text{ Tyr}^\bullet/\text{Tyr H} = 0.88 \text{ V}$) while the alkyl radicals ($E^\circ \text{ L}^\bullet/\text{LH} = 0.6 \text{ V}$) could not be able to perform that oxidation. Herein, we postulate that LOO[•] are capable of oxidizing tyrosine to •Tyr, therefore fueling the tyrosine oxidation pathway in hydrophobic biocompartments. To test this hypothesis, we have studied BTBE dimerization and nitration in PC liposomes of different unsaturation degree promoted by three different oxidation systems, namely peroxy nitrite, hemin and the peroxy radical donor 2,2'-azobis (2-amidinopropane) hydrochloride (ABAP) and their relationship with the lipid peroxidation process.

Experimental Procedures

Chemicals

Diethylentriaminepentaacetic acid (dtpa), manganese dioxide, sodium bicarbonate, potassium phosphate, L-tyrosine, 3-nitrotyrosine, α-tochopherol, 2-methyl-nitroso-propane (MNP), 1,1,3,3 tetra methoxypropane and hemin were purchased from SIGMA. *N*-t-BOC L-tyrosine *tert* butyl ester (BTBE), 3-nitro-*N*-t-BOC L-tyrosine *tert* butyl ester (3-nitro-BTBE) and 3,3'- di-*N*-t-BOC L-tyrosine *tert* butyl ester (3,3'-di-BTBE) were prepared and handled as previously (42). *N*-t-BOC L-phenylalanine *tert* butyl ester (BPBE) was synthesized for the first time using an identical procedure as the one previously described

for BTBE but starting from commercially available (SIGMA) L-phenylalanine-t-butylester (42). Stock BTBE solutions (1 M) were prepared in methanol immediately before use. 3,3'-dityrosine was synthesized by incubating 0.5 mM L-tyrosine, 0.2 mg/ml (4.5 μ M) horseradish peroxidase, and 500 μ M H₂O₂ in 50 mM phosphate buffer (pH 7.4) for 20 min at 25°C. The resulting mixture was centrifuged through a Centricon tube (molecular weight cutoff 5,000 Da) to remove the enzyme and the concentration of 3,3'-dityrosine obtained determined spectrophotometrically at 315 nm using an extinction coefficient of 5,700 M⁻¹ cm⁻¹ (pH 7.4) and 8,380 M⁻¹ cm⁻¹ (pH 9.9) (52). 1,2-dilauroyl-sn-glycero-3-phosphocholine (DLPC), 1-palmitoyl-2-linoleoyl-sn-glycero-3-phosphocholine (PLPC), egg yolk and soybean phosphatidylcholine (EYPC and SBPC) were from Avanti Polar Lipids. Organic solvents for synthesis of standards and chromatography were from Baker or Mallinckrodt. All other compounds were reagent grade.

Stock hemin solution was freshly prepared in 0.1 N NaOH and kept in the dark at 4° C until use. ABAP (2,2'-Azobis (2-amidinopropane) hydrochloride) was purchased from Wako Chemicals USA. A freshly stock solution (100 mM) was prepared in water and incubations were performed at 37°C for the indicated times.

Argon and nitrogen gas were purchased in AGA Chemical Co. (Uruguay).

All solutions were prepared with highly pure deionized nanopure water to minimize trace metal contamination.

Peroxynitrite synthesis and quantitation

Peroxynitrite was synthesized in a quenched-flow reactor from sodium nitrite (NaNO₂) and hydrogen peroxide (H₂O₂) under acidic conditions as described previously (53). The H₂O₂ remaining from the synthesis was eliminated by treating the stock solutions of peroxy nitrite with granular manganese dioxide, and the alkaline peroxy nitrite stock solution was kept at -20°C until use. Peroxy nitrite concentrations were determined spectrophotometrically at 302 nm ($\epsilon = 1670 \text{ M}^{-1} \text{ cm}^{-1}$) (44, 54). The nitrite concentration in the preparations was typically lower than 20% respect to peroxy nitrite. Control of nitrite levels revealed to be critical for obtaining reproducible data as, if present in excess, it can react with •OH and other oxidants and yield •NO₂ (41). In control experiments, peroxy nitrite was allowed to decompose to nitrate in 100 mM phosphate buffer, pH 7.4 before use, *i.e.*, “reverse order addition” of peroxy nitrite.

BTBE incorporation into liposomes and oxidizing systems

BTBE incorporation into liposomes was carried out as in (41, 42) with minor modifications. Briefly, a methanolic solution of BTBE (0.35 mM) was added to 35 mM PC lipids dissolved in chloroform. Under these conditions more than 98% BTBE was incorporated (42). The mixture was then dried under a stream of nitrogen gas. Previous studies from our group (41, 42) already indicated that BTBE incorporation yields and formation of oxidation products from peroxy nitrite were comparable in unilamellar and multilamellar liposomes and therefore not dependent on the membrane morphology. Therefore, due to the more simple preparation procedure, reported experiments were carried out mainly with multilamellar liposomes. Multilamellar liposomes were formed by thoroughly mixing the dried lipid with 100 mM sodium phosphate buffer (pH 7.4) plus 0.1 mM dtpa. For experiments with α -tocopherol-containing liposomes, α -tocopherol (in ethanol) was added at the desired concentration to the lipid solution in chloroform with or without BTBE and liposomes prepared thereafter as indicated above. Liposomes (30 mM PC and 0.3 mM BTBE) were exposed to peroxy nitrite, hemin or ABAP under different conditions throughout the work. BTBE and BTBE-derived products (*e.g.* 3-nitro-BTBE and 3,3'-di-BTBE) were extracted

with chloroform, methanol and 5 M NaCl as reported previously (1:2:4:0.4, sample : methanol : chloroform : NaCl v/v with recovery efficiencies for all compounds > 95% (42)). Samples were then dried and stored at -20°C. Immediately before HPLC separation, samples were resuspended in 100 µl of a mixture containing 85% methanol and 15% KPi (15 mM) pH 3. Experiments with liposomes were performed at 25°C, a temperature above the transition phase temperatures of the different liposomes and at 37°C when ABAP was used as an oxidant.

Oxidation systems

BTBE-containing PC liposomes were oxidized either by the addition of peroxynitrite, hemin or the organic peroxy radical donor ABAP. Peroxynitrite was added as a single bolus under vigorous vortexing ($t_{1/2}$ 2.5 s at 25°C (55)) or by slow infusion using a motor-driven syringe system (KD Scientific) under continuous stirring. Due to the addition of alkaline peroxynitrite solutions, the final pH was also checked at the end of the incubation to make sure that there were no significant variations (<0.1 pH units). Hemin was added directly to the PC liposomes; EYPC and SBPC liposomes always contain a basal level of pre-formed lipid hydroperoxides that serve as the redox substrate for hemin. Alternatively, *tert*-butyl hydroperoxide was used as hemin reactant in DLPC liposomes. Finally, in the case of ABAP, samples were incubated at 37°C during 2–3 hs to achieve a final ABAP concentration of 0–40 mM. ABAP-dependent oxygen consumption was measured using a high resolution oxymeter (Oroboros 2K) yielding a flux of 0.3 µM/min of peroxy radicals.

Experiments under low oxygen tension (*ca.* 5 µM) were carried out, by extensively purging samples under argon for 30 minutes.

Lipid peroxidation analysis

Malondialdehyde (MDA), a byproduct of lipid peroxidation, was measured as a thiobarbituric acid reactive substance at 532 nm ($\epsilon = 150,000 \text{ M}^{-1} \text{ cm}^{-1}$), as previously described (44). Calibration curves and assessment of malondialdehyde content were performed with known amounts of MDA obtained from the acid hydrolysis of 1,1,3,3 tetramethoxypropane in 20 % acetic acid pH 3.5. To prevent further peroxidation of lipids during assay procedures, 0.05% (w/v) of butylated hydroxytoluene (BHT) was added to the TBARS reagent. Lipid hydroperoxide formation was evaluated by the FOX assay (56). Briefly, 50 µl of the liposome sample was added to 950 µl of FOX reagent consisting in 100 mM xylenol orange, 250 mM Fe²⁺ (ferrous ammonium sulfate), 25 mM H₂SO₄, and 4 mM BHT in 90% (v/v) methanol. Reaction mixtures were incubated 1h at room temperature and absorbance was measured at 560 nm. Concentration of lipid hydroperoxides was estimated with the apparent extinction coefficient of 43,000 M⁻¹ cm⁻¹ (56).

Oxygen consumption during lipid peroxidation processes was measured by high resolution oxymetry using an Oxygraph 2K (Oroboros Instruments, Austria).

HPLC analysis

BTBE, 3-nitro-BTBE and 3,3'-di-BTBE were separated on a Agilent 1200 system equipped with UV-Vis and fluorescence detectors by reverse-phase HPLC using a Agilent Eclipse XDB-C18 5 µm column (150 mm length, 4.6 mm ID). Mobile phase A consisted in 15 mM phosphate buffer pH 3 and mobile phase B consisted in methanol. Chromatographic conditions were: flow 1ml / min; 75 % mobile phase B for 25 minutes, followed by a linear increase to 100% mobile phase B for 10 minutes. UV-Vis settings were for BTBE (280 nm, $\epsilon=1200 \text{ M}^{-1} \text{ cm}^{-1}$) and for 3-nitro-BTBE (360 nm, $\epsilon=1500 \text{ M}^{-1} \text{ cm}^{-1}$). 3,3'-di-BTBE was detected fluorimetrically at $\lambda_{\text{ex}} = 294 \text{ nm}$, $\lambda_{\text{em}} = 401 \text{ nm}$. Authentic 3-nitro-BTBE and 3,3'-di-BTBE were used as standards.

3-Nitrotyrosine and 3,3'-dityrosine were separated by reverse-phase HPLC, using a Partisil ODS-3 10 µm (250 mm length, 4.6 mm ID) C18 column as previously reported with minor modifications (41). Briefly, separation of tyrosine oxidation products was performed by isocratic RP-HPLC. Chromatographic conditions were: flow 1ml / min; 97% mobile phase A (KPi 15mM pH 3) and 3% mobile phase B (methanol) for 30 minutes. 3-Nitrotyrosine was measured by UV detection (280 nm and 360 nm) and 3,3'-dityrosine was measured fluorometrically ($\lambda_{\text{ex}} = 280 \text{ nm}$ and $\lambda_{\text{em}} = 400 \text{ nm}$). Authentic 3,3'-dityrosine and 3-nitro-Tyr were used as standards.

Artifactual BTBE or tyrosine nitration during the chromatographic separation procedure due to nitrite-dependent nitration at acidic pH were ruled out by appropriate controls using pre-decomposed peroxynitrite.

ESR-Spin Trapping measurements

ESR spectra were recorded at room temperature on a Bruker EMX spectrometer operating at 9.8 GHz. Typical spectrometer parameters were as follow: sweep width, 100 G; center field, 3505 G; time constant, 20.48 ms; scan time, 42 s; modulation amplitude, 1.0 G; modulation frequency, 100 kHz; receiver gain, 1×10^6 ; microwave power, 20 mW. Samples were subsequently transferred to a 50 µL capillary tube for ESR measurements.

MNP (20 mM) was used as spin trap; its photolysis may occur during the experiments and leads to the formation of a three line signal corresponding to the di-*tert*-butyl nitroxide radical, but it has a different a_N of 17.1 G. In order to minimize this, all liposomes preparations and solutions were covered with aluminum foil and spectra were recorded in the dark and therefore the signal due to photolysis was not seen under our experimental conditions.

General experimental conditions

Experiments were typically carried out in the presence of BTBE (0.3 mM) in PC liposomes (30 mM) in 100 mM sodium phosphate plus 0.1 mM dtpa, (pH 7.4) and 25°C unless otherwise stated.

Data analysis

All experiments reported herein were repeated a minimum of three times. Results are expressed as mean values with the corresponding standard deviations. Graphics and data analysis were performed using Origin 8.0.

RESULTS

Participation of lipid-derived radicals on BTBE oxidation

When BTBE-containing DLPC liposomes were treated with peroxynitrite (1 mM), 3-nitro-BTBE and 3,3'-di-BTBE were formed in yields of up to 2.5% and 0.01 % respect to initial peroxynitrite concentration respectively (Fig. 1A and B), in agreement with previous results (41, 57). Significant levels of both BTBE oxidation products were also formed in EYPC (Fig. 1) and SBPC, which contain a significant proportion of unsaturated fatty acids, ~ 24 and 57 % respectively. Thus, in spite of the fact that for EYPC and SBPC (30 mM) unsaturated fatty acids correspond to ~ 15 and 34 mM, respectively, a much larger concentration than that of BTBE (0.3 mM), the BTBE oxidation process was still operative.

To assess the participation of lipid-derived radicals in BTBE oxidation, experiments were also performed under low oxygen tensions (Fig. 1) which should result in an inhibition of LOO[•] formation (Eq. 2) in both saturated² (58) and unsaturated fatty acids. Indeed, under

these conditions, BTBE nitration and dimerization yields were substantially decreased either in saturated and unsaturated fatty acid-containing liposomes (Fig. 1A and B). In parallel, we evaluated lipid peroxidation in the samples by quantitating MDA, a well-known breakdown product of peroxidized lipids. Peroxynitrite caused MDA formation in BTBE-containing EYPC and SBPC liposomes (Fig. 1C), in agreement with our previous observations (41); importantly, MDA levels were reduced under low oxygen concentration, revealing the inhibition of the lipid peroxidation process. As expected, no MDA was detected in DLPC samples. Thus, in unsaturated fatty acid-containing liposomes (EYPC and SBPC), BTBE oxidation and lipid peroxidation occurred simultaneously and were both inhibited at low oxygen levels. Lipid hydroperoxide levels were significantly higher (over one order of magnitude) than those obtained for BTBE oxidation products, in agreement with the idea that lipid peroxidation is the main process within the membrane. On the other hand, when tyrosine (0.3 mM) was exposed to peroxy nitrite (1 mM) in 100 mM phosphate buffer (pH 7.3) 0.1 mM DTPA, oxygen did not influence tyrosine nitration and dimerization yields (~ 6 % and 0.25 %) yields respect peroxy nitrite, respectively) in aqueous phase (not shown). Overall, the data point to the formation of LOO[•] as key intermediates in the BTBE oxidation process.

Electron spin resonance (ESR)-spin trapping was used to detect the lipid-derived and BTBE phenoxy radicals formed during peroxy nitrite exposures using MNP as described previously (41, 59). In DLPC liposomes no ESR signal was obtained in the absence of BTBE when exposed to peroxy nitrite (Fig. 2, line a). On the other hand, BTBE-containing DLPC liposomes treated with peroxy nitrite resulted in an anisotropic three line signal, confirming the formation of a partially immobilized phenoxy radical in the interior of the membrane (Fig. 2, line b) and in agreement with our previous work (41, 60). When peroxy nitrite-treated BTBE containing DLPC liposomes were dissolved in ethanol (60), a sharper and clear three line signal was obtained which, despite of the low signal-to-noise ratio, allowed the determination of a hyperfine constant of 13.8 G; this is consistent with a MNP adduct with the one-electron oxidation of BTBE (61). In EYPC liposomes, peroxy nitrite caused the formation of a MNP adduct in the absence of BTBE, compatible with the formation of MNP-lipid alkyl (carbon-centered adduct) radical adducts (Fig. 2 line c) with an estimated hyperfine splitting constant $a_N \sim 15$ G (59). When BTBE was incorporated to liposomes, the signal was even larger (Fig. 2 line d), supporting the coexistence of lipid-derived and BTBE phenoxy radicals, and confirming the temporal association between the lipid peroxidation and BTBE oxidation processes. No ESR spectrum was obtained in DLPC or EYPC liposomes when treated with decomposed peroxy nitrite (Fig. 2 lines e and f) or if MNP was added after peroxy nitrite (Fig. 2 line g) or if peroxy nitrite was added to MNP only (without liposomes, not shown).

Slow infusion vs bolus addition of peroxy nitrite in lipid peroxidation and BTBE oxidation

Peroxy nitrite has a short half-life in 100 mM phosphate buffer, pH 7.4 and 25° C ($t_{1/2} 2.5$ s) due to the proton-catalyzed homolysis to •OH and •NO₂ in 30 % yields (55). Thus, addition of peroxy nitrite to reaction mixtures as a single bolus may result in high initial concentration of radicals and the extent of oxidation processes in target molecules not necessarily reflect the expected outcome in more biologically-relevant conditions where peroxy nitrite is formed as a continuous flow (62, 63). This consideration becomes particularly important in lipid peroxidation processes which depend on propagation reactions where an initial large flux of radicals will prematurely terminate the process. Thus, experiments were performed

²Saturated fatty acids (e.g. lauric acid in DLPC) will also react with •OH at fast rates ($k \sim 5 \times 10^9$ M⁻¹s⁻¹ (58)) to yield the alkyl radical. This can evolve to lauric acid peroxy radical, that, however, will not be capable of propagate a lipid peroxidation chain reaction in DLPC liposomes due to the lack of unsaturated fatty acids. Still, the peroxy radical could be potentially reactive with other targets such as BTBE (*vide infra*).

to study lipid peroxidation and BTBE oxidation yields with peroxynitrite addition as a single bolus or by slow infusion for up to 30 min (1 μ M/min). Peroxynitrite addition to BTBE-containing EYPC liposomes resulted in dose-dependent formation of MDA (Fig. 3 panel A); MDA yields were increased two to three fold when peroxynitrite was added as a slow infusion. Similarly, BTBE nitration and dimerization (Fig. 3, panels B, C and D) yields in both EYPC and DLPC by peroxynitrite infusion were up to three-fold higher than with bolus addition. Moreover, BTBE oxidation (Fig. 3, panel E) and MDA formation (not shown) yields in EYPC were significantly reduced under low oxygen tensions when peroxynitrite was added as a slow infusion. The data further support an association between the lipid peroxidation and BTBE oxidation processes.

Effect of phospholipid unsaturation degree in peroxynitrite-mediated BTBE oxidation

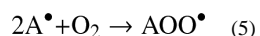
BTBE oxidation was studied as a function of fatty acid unsaturation by using liposomes containing variable mixtures of DLPC and PLPC. Nitration and dimerization yields were significant through all the phospholipid unsaturation range (0–100 %). A tendency towards increased BTBE oxidation yields was observed at around 40 % PLPC content, while a slight decrease was observed at 100 % PLPC. Thus, in spite of a largely variable content of unsaturated fatty acids in the liposomal mixtures (from 0 to 30 mM linolenic acid), BTBE oxidation was consistently present. Thus, the data support that a simple kinetic competition model, where unsaturated fatty acids simply outcompete BTBE for peroxynitrite-derived radicals does not apply, and that secondary reactions of lipid-derived radicals with BTBE must contribute to nitration and dimerization reactions (Fig. 4).

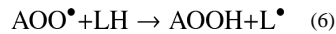
Hemin and ABAP-induced lipid peroxidation

To further demonstrate that lipid peroxidation processes are related with BTBE oxidation, we exposed BTBE-containing liposomes to two other oxidation systems, namely hemin and ABAP, both of which lead to the formation of LOO[•] in unsaturated fatty acid-containing liposomes. Free hemin readily interacts with membranes (64) and initiates lipid peroxidation in unsaturated liposomes by reaction with LOOH always present in variable extents in EYPC and SBPC (typical hydroperoxide content in well-stored preparations represent in our 30 mM liposome samples~ 45–80 μ M, 0.075–0.13 % of total unsaturated fatty acid as determined by the FOX assay). Hemin (Fe^{3+}) promotes the one-electron oxidation of LOOH to yield LOO[•] and hemin in the Fe^{2+} redox state (Scheme 1). In turn, the reduced hemin can generate LO[•] by reduction of LOOH.

Secondary reactions in the system generate variable amounts of, O₂^{•-}, H₂O₂ and heme-Fe⁴⁺=O that can amplify the process (64). In EYPC liposomes hemin induced 3,3'-di-BTBE and MDA formation in a dose-dependent manner (Fig. 5). On the other hand, in DLPC liposomes (saturated), where hemin can not cause lipid peroxidation, no formation of 3,3'-di-BTBE was detected. Thus, the data imply the participation of LOO[•] radicals formed from the reaction of hemin with lipid hydroperoxides (Scheme 1) in the BTBE dimerization process.

Secondly, we performed experiments using the organic peroxy radical donor, ABAP, which generates a flux of peroxy radicals by thermolysis.



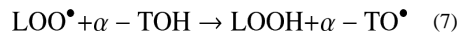


ABAP initiates lipid peroxidation in unsaturated fatty acid-containing liposomes such as EYPC, by the reaction of the ABAP-derived peroxy radicals (AOO^\bullet) with an unsaturated alkyl chain to yield the alkyl radical (L^\bullet) which then (Eqs. 4–6), after oxygen addition forms lipid peroxy radical. The addition of ABAP to BTBE-containing liposomes resulted in the formation of 3,3'-di-BTBE both in DLPC and EYPC liposomes (Table 1Fig. 6A), but MDA formation was observed in EYPC liposomes only. Thus, either ABAP-derived (in the DLPC experiment) or lipid-derived (in the EYPC one) peroxy radicals react with BTBE to yield BTBE-derived phenoxy radical and subsequently 3,3'-di-BTBE. Interestingly, samples treated with ABAP plus nitrite resulted in the formation of both 3,3'-di-BTBE and $3\text{-NO}_2\text{-BTBE}$ supporting that ABAP-derived peroxy radicals can also oxidize nitrite to $\bullet\text{NO}_2$ (Tables 1 and 2) (65). Low oxygen levels decreased BTBE oxidation yields induced by ABAP plus nitrite, both in DLPC and EYPC liposomes confirming the role of LOO^\bullet in the process. Control experiments with nitrite only showed no formation of BTBE oxidation products (Table 1).

To specifically address the reaction of organic peroxy radicals with tyrosine, we studied the effect of ABAP on free tyrosine oxidation in aqueous phase (Fig. 6B). Tyrosine exposure to ABAP-derived peroxy radicals resulted in the formation of 3,3'-di-tyrosine (Fig. 6B line b); when nitrite was added to the incubation mixture, both tyrosine oxidation products, 3-nitrotyrosine and 3,3'-dityrosine were formed (Fig. 6B, line c). Tyrosine nitration and dimerization yields were lower with free tyrosine in aqueous solution than those observed for BTBE in liposomes which suggest that tyrosine oxidation by peroxy radicals more easily occurs in non-polar environments.

Effect of α -tocopherol on BTBE oxidation and lipid peroxidation

α -tocopherol is a well known lipophilic chain breaking antioxidant that reacts with LOO^\bullet with a rate constant of $5 \times 10^5 \text{ M}^{-1} \text{ s}^{-1}$ (66) to yield lipid hydroperoxides and the stable α -tocopheroyl radical (Eq. 7):



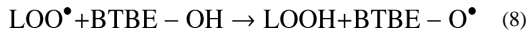
α -Tocopherol incorporated into EYPC liposomes inhibited peroxynitrite-mediated BTBE nitration (Fig. 7A), dimerization (not shown) and lipid peroxidation (Fig. 7B) in a dose-dependent manner. Interestingly, α -tocopherol also inhibited BTBE oxidation in DLPC liposomes, where no lipid peroxidation occurs. The effect of α -tocopherol is explained by the reaction between α -tocopherol with LOO^\bullet . In the case of DLPC, the reaction of α -tocopherol with $\bullet\text{NO}_2$ ($k = 1 \times 10^5 \text{ M}^{-1} \text{ s}^{-1}$ (67)) also becomes relevant to explain the inhibition of BTBE oxidation.

Oxygen consumption studies and kinetic determination of lipid peroxy radical reaction with BTBE

Experiments were performed to measure the oxygen consumption associated to lipid peroxidation initiated by hemin and ABAP and the potential chain breaking reaction of BTBE. If lipid peroxy radicals react to a significant extent with BTBE, then, the hydrophobic tyrosine analog should inhibit oxygen consumption. In EYPC (but not in DPLC) liposomes (in the absence of BTBE) a basal decrease in oxygen concentration is shown. Oxygen consumption is observed upon the addition of either ABAP or hemin (Fig. 8A), in agreement with the initiation and propagation phases of lipid peroxidation. In contrast, no further oxygen consumption was observed in DLPC liposomes after ABAP or

hemin addition (Fig. 8A). The incorporation of α -tocopherol to EYPC liposomes resulted in a significant decrease in oxidant-induced oxygen consumption rates (Fig. 8B). The extent of inhibition in oxygen consumption by α -tocopherol is compatible with the previously reported rate constants of LOO^\bullet with adjacent alkyl chains ($k = 36 \text{ M}^{-1}\text{s}^{-1}$) (68) and with α -tocopherol ($k = 5 \times 10^5 \text{ M}^{-1}\text{s}^{-1}$) (66). The inhibitory action of α -tocopherol was also observed if added exogenously during the time course of the oxygen consumption studies, but was less potent than when pre-incorporated, due the sub-optimal penetration in the preformed liposome structure within the time frame of the experiment. Remarkably, the incorporation of BTBE to the EYPC liposomes resulted in a dose-dependent inhibition of both hemin and ABAP-induced oxygen consumption rates, which is consistent with the reaction of BTBE with lipid-derived radicals (Fig. 8B). To discard subtle structural effects in the liposomal membranes due to BTBE incorporation, experiments were performed using a phenylalanine hydrophobic analog (BTPE) pre-incorporated to the liposomes (Fig. 8C). In this case, oxygen consumption rates were identical to the one observed in control EYPC (without BTBE), which is in agreement with a direct participation of the phenolic-OH moiety in the BTBE in reaction leading to inhibition of lipid peroxidation-dependent oxygen consumption, which is not present in the phenylalanine derivative (Fig. 8C).

The dose-dependent inhibition of oxygen consumption by increasing concentrations of pre-incorporated BTBE in EYPC liposomes was further analyzed in order to obtain an estimated second order rate constant for the reaction of LOO^\bullet with BTBE. A plot that relates the inhibition fraction in oxygen consumption as a function of BTBE concentration is in agreement with a direct competition of BTBE for the lipid peroxy radicals (Fig. 8D). These data allows the estimation of an apparent second order rate constant of $4.8 \times 10^3 \text{ M}^{-1}\text{s}^{-1}$ for the following reaction:



This rate constant value compares well with an independent determination considering the α -tocopherol studies. From data in Fig. 8 panels B and C, one concludes that 87 % inhibition is obtained with $5 \mu\text{M}$ α -tocopherol or 1 mM BTBE. Considering the stoichiometric factor $n = 2$ for α -tocopherol (69), thus, $2 \times k_{loc} [\alpha\text{-tocopherol}] = k_{BTBE} [\text{BTBE}]$, so $2 \times k_{loc} [\alpha\text{-tocopherol}] / [\text{BTBE}] = k_{BTBE} = 5 \times 10^3 \text{ M}^{-1}\text{s}^{-1}$.

In addition, both MDA and hydroperoxide yields were decreased in the presence of BTBE, in agreement with a reaction between BTBE and lipid peroxy radicals (Fig. 8E and F) and with the oxygen consumption data.

Discussion

Previously identified and biologically-relevant one-electron oxidants for tyrosine in aqueous environments include $\cdot\text{OH}$, $\text{CO}_3^{\bullet-}$ and $\cdot\text{NO}_2$, compounds I and II of hemeperoxidases and high oxidation states of transition metal centers (5). However, in the case of tyrosine oxidation in proteins associated to hydrophobic biocompartments such as membranes or lipoproteins a) some of the oxidants may not easily reach or permeate the lipid phase and b) unsaturated fatty acids, due to its reactivity and large concentration, constitute preferential targets for the initial oxidative attack. Thus, mechanisms by which tyrosine residues become dimerized and nitrated in hydrophobic biocompartments seem to have unique characteristics from those previously described in hydrophilic phases. In this work we have explored, using a validated model system of PC liposomes containing a hydrophobic tyrosine analog (BTBE), whether lipid-derived radicals generated during lipid peroxidation processes can mediate tyrosine oxidation to tyrosyl radical, the first step in the path to 3,3'-dityrosine or 3-nitrotyrosine.

Lipid peroxidation was initiated by three independent oxidation systems, namely peroxy nitrite, hemin and ABAP. Peroxy nitrite promotes lipid peroxidation and tyrosine nitration in hydrophobic compartments secondary to homolysis of peroxy nitrous acid (ONOOH) to $\bullet\text{OH}$ and $\bullet\text{NO}_2$ inside or at close proximity of the lipid phase (41, 44, 70). In EYPC, for instance, the large concentration ratio of unsaturated fatty acid/BTBE (50/1) and the participating rate constants (see Table 2), determine that the initial attack of peroxy nitrite-derived radicals occurs at the fatty acid moieties; this initial reaction yields the alkyl (pentadienyl) radical that upon oxygen addition evolves to LOO^\bullet which propagates the process (44). Alternatively, lipid-derived radicals were generated by the reaction of hemin with pre-existing lipid hydroperoxides to directly yield LOO^\bullet or by ABAP whose peroxy radical-derivative diffuses to the liposomes and reacts with unsaturated alkyl chains to initiate lipid peroxidation as well (71). Lipid peroxy radicals are known to react at fast rates with some phenolic compounds, including α -tocopherol and other dietary compounds that may exert antioxidant actions *in vitro* and *in vivo*. For example, linoleate peroxy radicals react with phenolic antioxidant compounds such as α -tocopherol, curcumin and quercetin with rate constants in the range $\sim 10^6 \text{ M}^{-1} \text{ s}^{-1}$ – $10^7 \text{ M}^{-1} \text{ s}^{-1}$ (72–75). In the case of tyrosine, another phenolic compound, the reaction with LOO^\bullet is thermodynamically possible; however, tyrosine is not a particularly good hydrogen donor and therefore the reaction may be kinetically hindered. Interestingly, hydrophobic phases may increase the reactivity of phenolic compounds such as tyrosine for LOO^\bullet (*see below*). Thus, extensive studies were performed herein to unambiguously show the existence of the LOO^\bullet reaction with the hydrophobic tyrosine analog BTBE³.

The evidence we have gathered herein to support the participation of LOO^\bullet in the tyrosine oxidation processes promoted by the three different tested oxidation systems can be summarized as follows: a) tyrosine (BTBE) oxidation was seen in significant extents in unsaturated fatty acid-containing PC liposomes, b) tyrosine oxidation in liposomes (but not in aqueous phase) was decreased under low oxygen concentrations, c) lipid-derived and tyrosyl radicals were simultaneously detected, d) α -tocopherol strongly inhibited tyrosine oxidation, e) BTBE (but not BPTE) partially inhibited lipid peroxidation processes, f) changes in the levels of tyrosine oxidation and lipid peroxidation products followed a parallel trend, g) the data are in agreement with an overall process involving the free radical mechanisms of lipid peroxidation and tyrosine oxidation plus a “connecting reaction” represented by one-electron oxidation of tyrosine by LOO^\bullet (Eq. 7) (see also Table 2).

In regards to the reactivity of peroxy radicals with tyrosine, the data showed that ABAP-derived peroxy radicals were already capable of oxidizing both BTBE in DLPC (saturated) liposomes as well as free tyrosine (Table 1 and Fig. 6), but reaction yields were much larger for BTBE, compatible with the concept that the reaction of phenolic compounds with oxidizing radicals is influenced by a kinetic solvent effect (76, 77). Indeed, different phenolic compounds (*e.g.* quercetin, epicatechin) react with peroxy radicals at similar rates than α -tocopherol in non-polar solvents but not in hydrogen-bonding solvents. In solvents that are strong hydrogen bond acceptors the rate constants of peroxy radicals with phenolic compounds dramatically decline and may even become undetectable⁴ (78). Polar solvents a) interfere with the intramolecular stabilization (H- bonding) of the phenoxy radical and b) generate steric hindrance for the approach of the peroxy radical to the solvent-complexed phenol, which reduces the rate constant of H-atom abstraction. Such considerations become

³Alkoxy radicals (LOO^\bullet) are also formed in lipid peroxidation processes *via* one-electron reduction of lipid hydroperoxides (48) or breakdown of tetroxide intermediates formed by the coupling of lipid two peroxy radicals; alkoxy radicals are far more potent oxidizing species than LOO^\bullet but mainly rearrange to epoxyallylic radicals (50) which in turn after coupling to O_2 become a secondary peroxy radical.

⁴For instance, a decrease by a factor of 36 in the k value has been observed for the reaction of α -tocopherol with cumylperoxy radicals when changing from hexane to *tert*-butyl alcohol (78).

important in heterogenous phases of lipid bilayers, where the localization of the phenolic groups will influence their effectiveness to trap peroxy radicals. In the case of LOO^{\bullet} generated in EYPC, an estimated second order rate constant for the reaction with BTBE was obtained by oxygen consumption studies, using two different approaches considering independent “primary targets”, namely unsaturated fatty acids ($k_{\text{LH}} \sim 10\text{--}50 \text{ M}^{-1}\text{s}^{-1}$ and α -tocopherol ($k_{\alpha\text{-toc}} = 5 \times 10^5 \text{ M}^{-1}\text{s}^{-1}$) (66)) (Fig. 8). The estimated k_{BTBE} of $4.8 \times 10^3 \text{ M}^{-1}\text{s}^{-1}$ is compatible with the redox properties of tyrosine and the lack of an “induction period” in oxygen consumption studies when lipid peroxidation was initiated in BTBE-containing liposomes; this moderate rate constant (1/200 of that of α -tocopherol), is still larger than that of LOO^{\bullet} with LH (e.g. the reaction of linoleic acid peroxy radical with linoleic acid, $k = 36 \text{ M}^{-1}\text{s}^{-1}$ in 70 % EtOH (68)). The reactions of halogenated organic peroxy radicals (known to be more reactive than lipid peroxy radicals) with tyrosine have been reported at alkaline pH, where most of the tyrosine is in the phenolate form ($pK_{\text{Tyr-OH}} \sim 10$), with values approaching $10^8 \text{ M}^{-1}\text{s}^{-1}$ (79). Oxidation of the protonated form of the phenol by peroxy radicals (as expected at neutral pH or when inside a hydrophobic structure) is significantly less favorable, in full agreement with the k_{BTBE} value in the range of $10^3 \text{ M}^{-1}\text{s}^{-1}$ obtained.

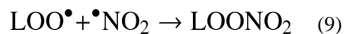
In a previous work (57), the nitration of a transmembrane peptide containing tyrosine in position eight from the C-terminus (*ca.* Y-8 at a depth of $\sim 20 \text{ \AA}$ from the surface) induced by the peroxy nitrite donor 3-morpholinosydnonimine hydrochloride (SIN-1) was progressively inhibited with increasing unsaturation degree of the DLPC:PLPC mixtures. A closer look to the data indicates that the extent of inhibition was significantly less than that predicted by a simple competition of Y-8 with unsaturated fatty acids (eg. at 40% liposome unsaturation and considering the reported rate constant values for hydroxyl radical and nitrogen dioxide-dependent fatty acid and tyrosine oxidation (Table 2), over 90 % inhibition of tyrosine oxidation would be expected but only 40 % inhibition was actually observed).

The relative yields of tyrosine dimerization and oxidation are largely affected by the biomembrane structure (41–43, 80), and we have estimated a diffusion coefficient (D) for BTBE in PC liposomes as *ca.* $5 \mu\text{m}^2 \text{ s}^{-1}$ (41). Thus, the rate constant value is lowered 100–200 fold ($k \sim 1\text{--}2 \times 10^6 \text{ M}^{-1} \text{ s}^{-1}$) with respect to the corresponding one of tyrosyl radicals ($k = 2.25 \times 10^8 \text{ M}^{-1} \text{ s}^{-1}$). Intermolecular tyrosine dimerization will be even less likely in integral peptides and proteins as D values become $>10^3\text{--}10^4$ times smaller than in solution depending on protein size (eg. $D \sim 0.1\text{--}0.5 \mu\text{m}^2 \text{ s}^{-1}$) (81, 82) and in line with the lack of tyrosine dimerization on transmembrane peptides treated with peroxy nitrite (57). On the other hand, $\bullet\text{NO}_2$ concentrates to some extent in hydrophobic environments (83), and the D value ($D \bullet\text{NO}_2$) is $\sim 1500 \mu\text{m}^2 \text{ s}^{-1}$, very close to that of the aqueous phase of $4500 \mu\text{m}^2 \text{ s}^{-1}$ (84), thus nitration in membranes is not kinetically impeded, a concept that is in perfect agreement with the large 3-nitro- BTBE/3,3’diBTBE ratios found during peroxy nitrite exposures.

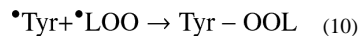
Significant evidence supports that lipid peroxidation and tyrosine oxidation processes are associated in oxidative-stress related processes and pathophysiology (31, 43, 85, 86) for instance, membrane protein tyrosine (and BTBE) oxidation and nitration were evidenced in red blood cells exposed to peroxy nitrite, in a process that was inhibited under low oxygen tensions (43). In a related way, accumulation of protein 3-nitrotyrosine and 4-hydroxynonenal protein adducts have been simultaneously detected in liver and kidney in a model of type I diabetes where peroxy nitrite has been identified as a key mediator of lipid peroxidation (86). Future work should address whether both processes *in vivo* are mechanistically linked as suggested by our *in vitro* model studies. Our data also indicate that α -tocopherol can potently modulate tyrosine oxidation yields in membranes by inhibiting lipid peroxidation. In this regard, it is important to consider that the extent of inhibition is a function of α -tocopherol levels that under biologically-relevant conditions (*ca.* 1 molecule

of α -tocopherol per 100–1000 molecules of membrane phospholipid; (87) may not be sufficient to fully prevent tyrosine oxidation events in either biomembranes (43, 86) or model membranes (this work, see Fig. 7A at 0–0.3 mM α -tocopherol for 30 mM DLPC). Thus, we predict that an increase of cell/tissue levels of α -tocopherol should result in attenuation of protein tyrosine oxidation both in biomembranes and lipoproteins.

In addition to lipid peroxidation products, other side reactions take place on lipid radical intermediates when peroxy nitrite and/or $\bullet\text{NO}_2$ are present leading to the formation of small amounts of nitrated lipids (88) (Eq. 9)



Additionally, a termination reaction between $\bullet\text{LOO}$ and $\bullet\text{Tyr}$ may occur yielding Diels Alder-type structures (89) (Eq. 10):



Membrane phospholipids have a low D value is (D_{PL} ca. $0.5\text{--}1 \mu\text{m}^2 \text{s}^{-1}$; (81)), but due to their abundance the formation of tyrosyl-phospholipid adducts is at least probable and deserves investigation in further studies.

In summary, the data presented herein support that $\bullet\text{LOO}$ participates in tyrosine oxidation processes in hydrophobic biocompartments and provides a new mechanistic insight to understand protein nitration in lipoproteins and biomembranes (Fig. 9). Notably, cell and tissue oxygen levels become a previously unrecognized factor that will critically influence tyrosine oxidation yields *via* the intermediacy of lipid peroxyl radicals.

Acknowledgments

This work was supported by grants from the Howard Hughes Medical Institute and International Centre for Genetic Engineering and Biotechnology to RR, National Institutes of Health to BK and RR (2 R01HI063119-05) and Agencia Nacional de Investigación e Innovación (ANII) / Fondo Clemente Estable to SB (FCE_362). SB was partially supported by a fellowship of ANII. RR is a Howard Hughes International Research Scholar.

Abbreviations

BTBE	<i>N</i> -t-BOC L-tyrosine <i>tert</i> butyl ester
BPBE	<i>N</i> -t-BOC L-phenylalanine <i>tert</i> butyl ester
DLPC	1,2- Dilauroyl- <i>sn</i> -glycero-3-phosphocholine
PLPC	1-palmitoyl-2-linoleoyl- <i>sn</i> -glycero-3-phosphocholine
EYPC	egg chicken yolk L- α -phosphatidylcholine
SBPC	soybean-L- α -phosphatidylcholine
dtpa	diethylentriaminepentaacetic acid
$\bullet\text{NO}$	nitric oxide
$\text{O}_2\bullet^-$	Superoxide
3-nitro-Tyr	3-nitrotyrosine
$\bullet\text{Tyr}$	tyrosyl radical

PC	Phosphatidylcholine
RP-HPLC	reverse-phase high performance liquid chromatography
ABAP	2,2'-Azobis (2-amidinopropane) hydrochloride
MDA	Malondialdehyde
FOX	Ferrous oxide-xylenol orange assay
LOO[•]	lipid peroxy radical
LO[•]	lipid alkoxyl radical
TBARS	thiobarbituric-acid reactive species
ESR	electron spin resonance
BHT	butylated hydroxytoluene and MNP (2-methyl nitrosopropane)
BOC	butoxypyrocarbonate

References

1. Bodaness RS, Leclair M, Zigler JS Jr. An analysis of the H₂O₂-mediated crosslinking of lens crystallins catalyzed by the heme-undecapeptide from cytochrome c. *Arch Biochem Biophys*. 1984; 231:461–469. [PubMed: 6732243]
2. Giulivi C, Traaseth NJ, Davies KJ. Tyrosine oxidation products: analysis and biological relevance. *Amino Acids*. 2003; 25:227–232. [PubMed: 14661086]
3. Heinecke JW. Tyrosyl radical production by myeloperoxidase: a phagocyte pathway for lipid peroxidation and dityrosine cross-linking of proteins. *Toxicology*. 2002; 177:11–22. [PubMed: 12126792]
4. Hsiai TK, Hwang J, Barr ML, Correa A, Hamilton R, Alavi M, Rouhanizadeh M, Cadenas E, Hazen SL. Hemodynamics influences vascular peroxynitrite formation: Implication for low-density lipoprotein apo-B-100 nitration. *Free Radic Biol Med*. 2007; 42:519–529. [PubMed: 17275684]
5. Radi R. Nitric oxide, oxidants, and protein tyrosine nitration. *Proc Natl Acad Sci U S A*. 2004; 101:4003–4008. [PubMed: 15020765]
6. Ischiropoulos H. Biological Selectivity and Functional Aspects of Protein Tyrosine Nitration. *Biochem. Biophys. Res. Commun.* 2003; 305:776–783. [PubMed: 12763060]
7. Peluffo G, Radi R. Biochemistry of protein tyrosine nitration in cardiovascular pathology. *Cardiovasc Res*. 2007; 75:291–302. [PubMed: 17544386]
8. Reynolds MR, Berry RW, Binder LI. Nitration in neurodegeneration: deciphering the "Hows" "nYs". *Biochemistry*. 2007; 46:7325–7336. [PubMed: 17542619]
9. Shishgehbor MH, Aviles RJ, Brennan ML, Fu X, Goormastic M, Pearce GL, Gokce N, Keaney JF Jr, Penn MS, Sprecher DL, Vita JA, Hazen SL. Association of nitrotyrosine levels with cardiovascular disease and modulation by statin therapy. *Jama*. 2003; 289:1675–1680. [PubMed: 12672736]
10. Beckman JS, Ischiropoulos H, Zhu L, van der Woerd M, Smith C, Chen J, Harrison J, Martin JC, Tsai M. Kinetics of superoxide dismutase- and iron-catalyzed nitration of phenolics by peroxynitrite. *Arch Biochem Biophys*. 1992; 298:438–445. [PubMed: 1416975]
11. Quijano C, Hernandez-Saavedra D, Castro L, McCord JM, Freeman BA, Radi R. Reaction of peroxynitrite with Mn-superoxide dismutase. Role of the metal center in decomposition kinetics and nitration. *J Biol Chem*. 2001; 276:11631–11638. [PubMed: 11152462]
12. Quint P, Reutzel R, Mikulski R, McKenna R, Silverman DN. Crystal structure of nitrated human manganese superoxide dismutase: mechanism of inactivation. *Free Radic Biol Med*. 2006; 40:453–458. [PubMed: 16443160]
13. Pehar M, Vargas MR, Robinson KM, Cassina P, Diaz-Amarilla PJ, Hagen TM, Radi R, Barbeito L, Beckman JS. Mitochondrial superoxide production and nuclear factor erythroid 2-related factor

- 2 activation in p75 neurotrophin receptor-induced motor neuron apoptosis. *J Neurosci*. 2007; 27:7777–7785. [PubMed: 17634371]
14. Batthyany C, Souza JM, Duran R, Cassina A, Cervenansky C, Radi R. Time course and site(s) of cytochrome c tyrosine nitration by peroxynitrite. *Biochemistry*. 2005; 44:8038–8046. [PubMed: 15924423]
15. Cassina AM, Hodara R, Souza JM, Thomson L, Castro L, Ischiropoulos H, Freeman BA, Radi R. Cytochrome c nitration by peroxynitrite. *J Biol Chem*. 2000; 275:21409–21415. [PubMed: 10770952]
16. Souza JM, Peluffo G, Radi R. Protein tyrosine nitration--functional alteration or just a biomarker? *Free Radic Biol Med*. 2008; 45:357–366. [PubMed: 18460345]
17. Estevez AG, Crow JP, Sampson JB, Reiter C, Zhuang Y, Richardson GJ, Tarpey MM, Barbeito L, Beckman JS. Induction of nitric oxide-dependent apoptosis in motor neurons by zinc- deficient superoxide dismutase. *Science*. 1999; 286:2498–2500. [PubMed: 10617463]
18. Ischiropoulos H, Beckman JS. Oxidative stress and nitration in neurodegeneration: cause, effect, or association? *J Clin Invest*. 2003; 111:163–169. [PubMed: 12531868]
19. Radi R, Peluffo G, Alvarez MN, Naviliat M, Cayota A. Unraveling peroxynitrite formation in biological systems. *Free Radic Biol Med*. 2001; 30:463–488. [PubMed: 11182518]
20. Alvarez B, Ferrer-Sueta G, Freeman BA, Radi R. Kinetics of peroxynitrite reaction with amino acids and human serum albumin. *J Biol Chem*. 1999; 274:842–848. [PubMed: 9873023]
21. Ferrer-Sueta G, Radi R. Chemical biology of peroxynitrite: kinetics, diffusion, and radicals. *ACS Chem Biol*. 2009; 4:161–177. [PubMed: 19267456]
22. Bartesaghi S, Ferrer-Sueta G, Peluffo G, Valez V, Zhang H, Kalyanaraman B, Radi R. Protein tyrosine nitration in hydrophilic and hydrophobic environments. *Amino Acids*. 2007; 32:501–515. [PubMed: 17077966]
23. Santos CX, Bonini MG, Augusto O. Role of the carbonate radical anion in tyrosine nitration and hydroxylation by peroxynitrite. *Arch Biochem Biophys*. 2000; 377:146–152. [PubMed: 10775454]
24. Bian K, Gao Z, Weisbrodt N, Murad F. The nature of heme/iron-induced protein tyrosine nitration. *Proc Natl Acad Sci U S A*. 2003; 100:5712–5717. [PubMed: 12709594]
25. Hazen SL, Zhang R, Shen Z, Wu W, Podrez EA, MacPherson JC, Schmitt D, Mitra SN, Mukhopadhyay C, Chen Y, Cohen PA, Hoff HF, Abu-Soud HM. Formation of nitric oxide-derived oxidants by myeloperoxidase in monocytes: pathways for monocyte-mediated protein nitration and lipid peroxidation In vivo. *Circ Res*. 1999; 85:950–958. [PubMed: 10559142]
26. Wu W, Chen Y, Hazen SL. Eosinophil peroxidase nitrates protein tyrosyl residues. Implications for oxidative damage by nitrating intermediates in eosinophilic inflammatory disorders. *J Biol Chem*. 1999; 274:25933–25944. [PubMed: 10464338]
27. Souza JM, Daikhin E, Yudkoff M, Raman CS, Ischiropoulos H. Factors determining the selectivity of protein tyrosine nitration. *Arch Biochem Biophys*. 1999; 371:169–178. [PubMed: 10545203]
28. Abriata LA, Cassina A, Tortora V, Marin M, Souza JM, Castro L, Vila AJ, Radi R. Nitration of solvent-exposed tyrosine 74 on cytochrome c triggers heme iron-methionine 80 bond disruption. Nuclear magnetic resonance and optical spectroscopy studies. *J Biol Chem*. 2009; 284:17–26. [PubMed: 18974097]
29. Mallozzi C, Di Stasi AM, Minetti M. Peroxynitrite modulates tyrosine-dependent signal transduction pathway of human erythrocyte band 3. *Faseb J*. 1997; 11:1281–1290. [PubMed: 9409547]
30. Robaszkiewicz A, Bartosz G, Soszynski M. N-chloroamino acids cause oxidative protein modifications in the erythrocyte membrane. *Mech Ageing Dev*. 2008; 129:572–579. [PubMed: 18586303]
31. Velsor LW, Ballinger CA, Patel J, Postlethwait EM. Influence of epithelial lining fluid lipids on NO(2)-induced membrane oxidation and nitration. *Free Radic Biol Med*. 2003; 34:720–733. [PubMed: 12633749]
32. Kaplan P, Tatarkova Z, Racay P, Lehotsky J, Pavlikova M, Dobrota D. Oxidative modifications of cardiac mitochondria and inhibition of cytochrome c oxidase activity by 4-hydroxynonenal. *Redox Rep*. 2007; 12:211–218. [PubMed: 17925093]

33. Murray J, Taylor SW, Zhang B, Ghosh SS, Capaldi RA. Oxidative damage to mitochondrial complex I due to peroxynitrite: identification of reactive tyrosines by mass spectrometry. *J Biol Chem.* 2003; 278:37223–37230. [PubMed: 12857734]
34. Poderoso JJ. The formation of peroxynitrite in the applied physiology of mitochondrial nitric oxide. *Arch Biochem Biophys.* 2009; 484:214–220. [PubMed: 19159609]
35. Xu S, Ying J, Jiang B, Guo W, Adachi T, Sharov V, Lazar H, Menzoian J, Knyushko TV, Bigelow DJ, Schoneich C, Cohen RA. Detection of Sequence-Specific Tyrosine Nitration of Manganese SOD and SERCA in Cardiovascular Disease and Aging. *AJP-Heart.* 2006; 290:2220–2227.
36. Shao B, Bergt C, Fu X, Green P, Voss JC, Oda MN, Oram JF, Heinecke JW. Tyrosine 192 in apolipoprotein A-I is the major site of nitration and chlorination by myeloperoxidase, but only chlorination markedly impairs ABCA1-dependent cholesterol transport. *J Biol Chem.* 2005; 280:5983–5993. [PubMed: 15574409]
37. Zhou W, Milder JB, Freed CR. Transgenic mice overexpressing tyrosine-to-cysteine mutant human alpha-synuclein: a progressive neurodegenerative model of diffuse Lewy body disease. *J Biol Chem.* 2008; 283:9863–9870. [PubMed: 18238775]
38. Vadseth C, Souza JM, Thomson L, Seagraves A, Nagaswami C, Scheiner T, Torbet J, Vilaire G, Bennett JS, Murciano JC, Muzykantov V, Penn MS, Hazen SL, Weisel JW, Ischiropoulos H. Prothrombotic state induced by posttranslational modification of fibrinogen by reactive nitrogen species. *J Biol Chem.* 2004; 279:8820–8826. [PubMed: 14681238]
39. Lizarbe TR, Garcia-Rama C, Tarin C, Saura M, Calvo E, Lopez JA, Lopez-Otin C, Folgueras AR, Lamas S, Zaragoza C. Nitric oxide elicits functional MMP-13 protein-tyrosine nitration during wound repair. *FASEB J.* 2008; 22:3207–3215. [PubMed: 18495757]
40. Moller MN, Li Q, Lancaster JR Jr, Denicola A. Acceleration of nitric oxide autoxidation and nitrosation by membranes. *IUBMB Life.* 2007; 59:243–248. [PubMed: 17505960]
41. Bartesaghi S, Valez V, Trujillo M, Peluffo G, Romero N, Zhang H, Kalyanaraman B, Radi R. Mechanistic Studies of Peroxynitrite-Mediated Tyrosine Nitration in Membranes Using the Hydrophobic Probe *N*-t-BOC-L-tyrosine *tert*-Butyl Ester. *Biochemistry.* 2006; 45:6813–6825. [PubMed: 16734418]
42. Zhang H, Joseph J, Feix J, Hogg N, Kalyanaraman B. Nitration and oxidation of a hydrophobic tyrosine probe by peroxynitrite in membranes: comparison with nitration and oxidation of tyrosine by peroxynitrite in aqueous solution. *Biochemistry.* 2001; 40:7675–7686. [PubMed: 11412121]
43. Romero N, Peluffo G, Bartesaghi S, Zhang H, Joseph J, Kalyanaraman B, Radi R. Incorporation of the hydrophobic probe N-t-BOC-L-tyrosine *tert*-butyl ester to red blood cell membranes to study peroxynitrite-dependent reactions. *Chem Res Toxicol.* 2007; 20:1638–1648. [PubMed: 17941688]
44. Radi R, Beckman JS, Bush KM, Freeman BA. Peroxynitrite-induced membrane lipid peroxidation: the cytotoxic potential of superoxide and nitric oxide. *Arch Biochem Biophys.* 1991; 288:481–487. [PubMed: 1654835]
45. Buxton GV, Greenstock CL, Helman WP, Ross AB. Critical Review of Rate Constants for Reactions of Hydrated Electrons, Hydrogen Atoms and Hydroxyl Radicals (.OH/.O-) in Aqueous Solution. *J Phys Chem Ref Data.* 1988; 17
46. Prutz WA, Monig H, Butler J, Land EJ. Reactions of nitrogen dioxide in aqueous model systems: oxidation of tyrosine units in peptides and proteins. *Arch Biochem Biophys.* 1985; 243:125–134. [PubMed: 4062299]
47. Pryor WA, Lightsey JW. Mechanisms of Nitrogen Dioxide Reactions: Initiation of Lipid Peroxidation and the Production of Nitrous Acid. *Science.* 1981; 214:435–437. [PubMed: 17730242]
48. Lee SH, Oe T, Blair IA. Vitamin C-induced decomposition of lipid hydroperoxides to endogenous genotoxins. *Science.* 2001; 292:2083–2086. [PubMed: 11408659]
49. Niki E, Yoshida Y, Saito Y, Noguchi N. Lipid peroxidation: mechanisms, inhibition, and biological effects. *Biochem Biophys Res Commun.* 2005; 338:668–676. [PubMed: 16126168]
50. Wilcox AL, Marnett LJ. Polyunsaturated fatty acid alkoxyl radicals exist as carbon-centered epoxyallylic radicals: a key step in hydroperoxide-amplified lipid peroxidation. *Chem Res Toxicol.* 1993; 6:413–416. [PubMed: 8374035]

51. Spiteller G. Peroxyl radicals: inductors of neurodegenerative and other inflammatory diseases. Their origin and how they transform cholesterol, phospholipids, plasmalogens, polyunsaturated fatty acids, sugars, and proteins into deleterious products. *Free Radic Biol Med.* 2006; 41:362–387. [PubMed: 16843819]
52. Malencik DA, Sprouse JF, Swanson CA, Anderson SR. Dityrosine: preparation, isolation, and analysis. *Anal Biochem.* 1996; 242:202–213. [PubMed: 8937563]
53. Radi R, Beckman JS, Bush KM, Freeman BA. Peroxynitrite oxidation of sulphydryls. The cytotoxic potential of superoxide and nitric oxide. *J Biol Chem.* 1991; 266:4244–4250. [PubMed: 1847917]
54. Beckman JS, Beckman TW, Chen J, Marshall PA, Freeman BA. Apparent hydroxyl radical production by peroxy nitrite: implications for endothelial injury from nitric oxide and superoxide. *Proc Natl Acad Sci U S A.* 1990; 87:1620–1624. [PubMed: 2154753]
55. Koppenol WH, Moreno JJ, Pryor WA, Ischiropoulos H, Beckman JS. Peroxynitrite, a cloaked oxidant formed by nitric oxide and superoxide. *Chem Res Toxicol.* 1992; 5:834–842. [PubMed: 1336991]
56. Jiang ZY, Woppard AC, Wolff SP. Lipid hydroperoxide measurement by oxidation of Fe²⁺ in the presence of xylene orange. Comparison with the TBA assay and an iodometric method. *Lipids.* 1991; 26:853–856. [PubMed: 1795606]
57. Zhang H, Bhargava K, Keszler A, Feix J, Hogg N, Joseph J, Kalyanaraman B. Transmembrane nitration of hydrophobic tyrosyl peptides. Localization, characterization, mechanism of nitration, and biological implications. *J Biol Chem.* 2003; 278:8969–8978. [PubMed: 12519728]
58. Barber DJW, Thomas JK. Reactions of radicals with lecithin bilayers. *Radiation Research.* 1978; 74:51–65.
59. Feix JB, Kalyanaraman B. Spin trapping of lipid-derived radicals in liposomes. *Biochim Biophys Acta.* 1989; 992:230–235. [PubMed: 2547451]
60. Bartesaghi S, Peluffo G, Zhang H, Joseph J, Kalyanaraman B, Radi R. Tyrosine nitration, dimerization, and hydroxylation by peroxy nitrite in membranes as studied by the hydrophobic probe N-t-BOC-l-tyrosine tert-butyl ester. *Methods Enzymol.* 2008; 441:217–236. [PubMed: 18554537]
61. Mossoba M, Makino K, Riesz P. Photoionization of aromatic amino acids in aqueous solutions. A spin-trapping and electron spin resonance study. *J Phys Chem.* 1982; 86:3478–3483.
62. Goldstein S, Czapski G, Lind J, Merenyi G. Tyrosine nitration by simultaneous generation of (.)NO and O-(2) under physiological conditions. How the radicals do the job. *J Biol Chem.* 2000; 275:3031–3036. [PubMed: 10652282]
63. Rubbo H, Denicola A, Radi R. Peroxynitrite inactivates thiol-containing enzymes of Trypanosoma cruzi energetic metabolism and inhibits cell respiration. *Arch Biochem Biophys.* 1994; 308:96–102. [PubMed: 8311481]
64. Kalyanaraman B, Mottley C, Mason RP. A direct electron spin resonance and spin-trapping investigation of peroxy free radical formation by hematin/hydroperoxide systems. *J Biol Chem.* 1983; 258:3855–3858. [PubMed: 6300059]
65. El-Agamy A. Laser flash photolysis of new water-soluble peroxy radical precursor. *Journal of Photochemistry and Photobiology A: Chemistry.* 2009; 203:13–17.
66. Niki E, Saito T, Kawakami A, Kamiya Y. Inhibition of oxidation of methyl linoleate in solution by vitamin E and vitamin C. *J Biol Chem.* 1984; 259:4177–4182. [PubMed: 6706998]
67. Davies MJ, Forni LG, Willson RL. Vitamin E analogue Trolox C. E.s.r. and pulse-radiolysis studies of free-radical reactions. *Biochem J.* 1988; 255:513–522. [PubMed: 2849418]
68. Gebicki JM, Bielski BHJ. *J Am Chem Soc.* 1981; 103:7020–7025.
69. Wayner DD, Burton GW, Ingold KU, Locke S. Quantitative measurement of the total, peroxy radical-trapping antioxidant capability of human blood plasma by controlled peroxidation. The important contribution made by plasma proteins. *FEBS Lett.* 1985; 187:33–37. [PubMed: 4018255]
70. Szabo C, Ischiropoulos H, Radi R. Peroxynitrite: biochemistry, pathophysiology and development of therapeutics. *Nat Rev Drug Discov.* 2007; 6:662–680. [PubMed: 17667957]

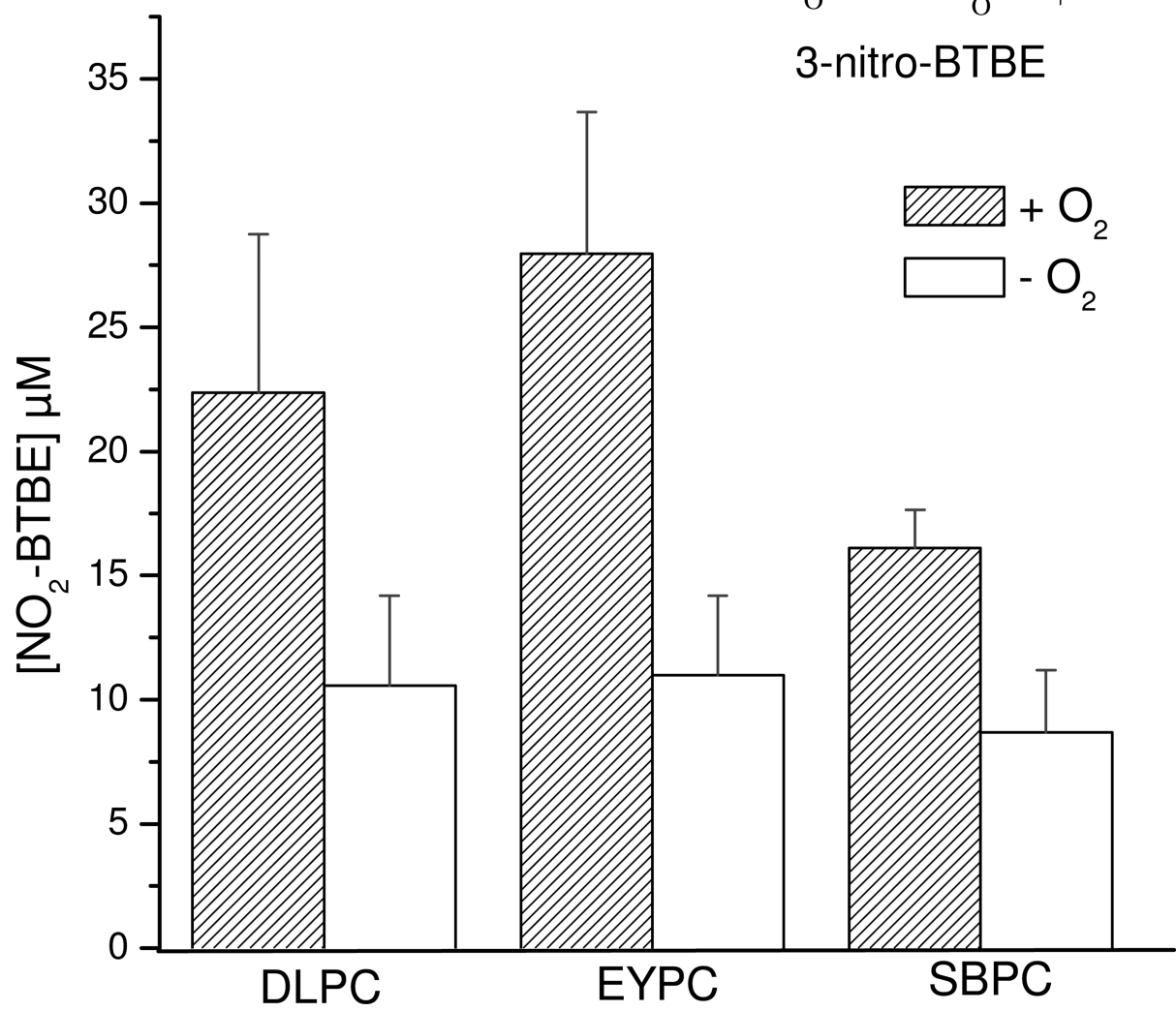
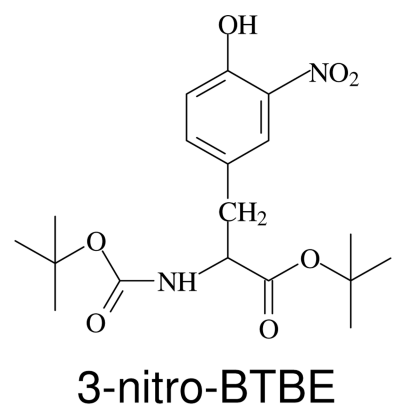
71. Rubbo H, Radi R, Anselmi D, Kirk M, Barnes S, Butler J, Eiserich JP, Freeman BA. Nitric oxide reaction with lipid peroxy radicals spares alphatocopherol during lipid peroxidation. Greater oxidant protection from the pair nitric oxide/alpha-tocopherol than alpha-tocopherol/ascorbate. *J Biol Chem.* 2000; 275:10812–10818. [PubMed: 10753874]
72. Erben-Russ M, Bors W, Saran M. Reactions of linoleic acid peroxy radicals with phenolic antioxidants: a pulse radiolysis study. *Int J Radiat Biol Relat Stud Phys Chem Med.* 1987; 52:393–412. [PubMed: 3497895]
73. Pedrielli P, Pedulli GF, Skibsted LH. Antioxidant mechanism of flavonoids. Solvent effect on rate constant for chain-breaking reaction of quercetin and epicatechin in autoxidation of methyl linoleate. *J Agric Food Chem.* 2001; 49:3034–3040. [PubMed: 11410005]
74. Priyadarsini KI. Free radical reactions of curcumin in membrane models. *Free Radic Biol Med.* 1997; 23:838–843. [PubMed: 9378362]
75. Priyadarsini KI, Guha SN, Rao MN. Physico-chemical properties and antioxidant activities of methoxy phenols. *Free Radic Biol Med.* 1998; 24:933–941. [PubMed: 9607603]
76. Amorati R, Catarzi F, Menichetti S, Pedulli GF, Viglianisi C. Effect of ortho-SR groups on O-H bond strength and H-atom donating ability of phenols: a possible role for the Tyr-Cys link in galactose oxidase active site? *J Am Chem Soc.* 2008; 130:237–244. [PubMed: 18072772]
77. Foti M, Ruberto G. Kinetic solvent effects on phenolic antioxidants determined by spectrophotometric measurements. *J Agric Food Chem.* 2001; 49:342–348. [PubMed: 11170597]
78. Valgimigli L, Banks JT, Lusztyk J, Ingold KU. Solvent Effects on the Antioxidant Activity of Vitamin E(1). *J Org Chem.* 1999; 64:3381–3383. [PubMed: 11674452]
79. Kapoor SK, Gopinathan C. Reactions of halogenated organic peroxy radicals with various purine derivatives, tyrosine and thymine: a pulse radiolysis study. *International of Chemical Kinetics.* 1992; 24:1035–1042.
80. Lide, DR. *Handbook of Chemistry and Physics.* 71st ed ed.. Boca Raton, FL: 1990.
81. Sackmann E, Trauble H, Galla H, Overath P. Lateral Diffusion, Protein Mobility and Phase Transitions in *Escherichia coli* Membranes. A Spin Label Study. *Biochemistry.* 1973; 12:5360–5369. [PubMed: 4357340]
82. Vanderkooi J, Fischkoff S, Chance B, Cooper RA. Fluorescent probe analysis of the lipid architecture of natural and experimental cholesterol-rich membranes. *Biochemistry.* 1974; 13:1589–1595. [PubMed: 4831349]
83. Moller MN, Li Q, Vitturi DA, Robinson JM, Lancaster JR Jr, Denicola A. Membrane "lens" effect: focusing the formation of reactive nitrogen oxides from the *NO/O₂ reaction. *Chem Res Toxicol.* 2007; 20:709–714. [PubMed: 17388608]
84. Moller M, Botti H, Bathany C, Rubbo H, Radi R, Denicola A. Direct measurement of nitric oxide and oxygen partitioning into liposomes and low density lipoprotein. *J Biol Chem.* 2005; 280:8850–8854. [PubMed: 15632138]
85. Hamilton RT, Asatryan L, Nilsen JT, Isas JM, Gallaher TK, Sawamura T, Hsiai TK. LDL protein nitration: implication for LDL protein unfolding. *Arch Biochem Biophys.* 2008; 479:1–14. [PubMed: 18713619]
86. Stadler K, Bonini MG, Dallas S, Jiang J, Radi R, Mason RP, Kadiiska MB. Involvement of inducible nitric oxide synthase in hydroxyl radical-mediated lipid peroxidation in streptozotocin-induced diabetes. *Free Radic Biol Med.* 2008; 45:866–874. [PubMed: 18620046]
87. Atkinson J, Epand RF, Epand RM. Tocopherols and tocotrienols in membranes: a critical review. *Free Radic Biol Med.* 2008; 44:739–764. [PubMed: 18160049]
88. Rubbo H, Radi R, Trujillo M, Telleri R, Kalyanaraman B, Barnes S, Kirk M, Freeman BA. Nitric oxide regulation of superoxide and peroxynitrite-dependent lipid peroxidation. Formation of novel nitrogen-containing oxidized lipid derivatives. *J Biol Chem.* 1994; 269:26066–26075. [PubMed: 7929318]
89. Masuda T, Bando H, Maekawa T, Takeda Y, Yamaguchi H. A Novel Radical Terminated Compound Produced in the Antioxidation Process of Curcumin Against Oxidation of a Fatty Acid Ester. *Tetrahedron Lett.* 2000; 41:2157–2160.
90. Solar S, Solar W, Getoff N. Reactivity of OH with tyrosine in aqueous solution studie by pulse radiolysis. *J Phys Chem.* 1984; 88:2091–2095.

91. Jin F, Leitich J, Sonntag Cv. J Chem Soc Perkin Trans. 1993; 2:1583–1588.
92. Babbs CF, Steiner MG. Simulation of free radical reactions in biology and medicine: a new two-compartment kinetic model of intracellular lipid peroxidation. Free Radic Biol Med. 1990; 8:471–485. [PubMed: 2174816]

\$watermark-text

\$watermark-text

\$watermark-text

A

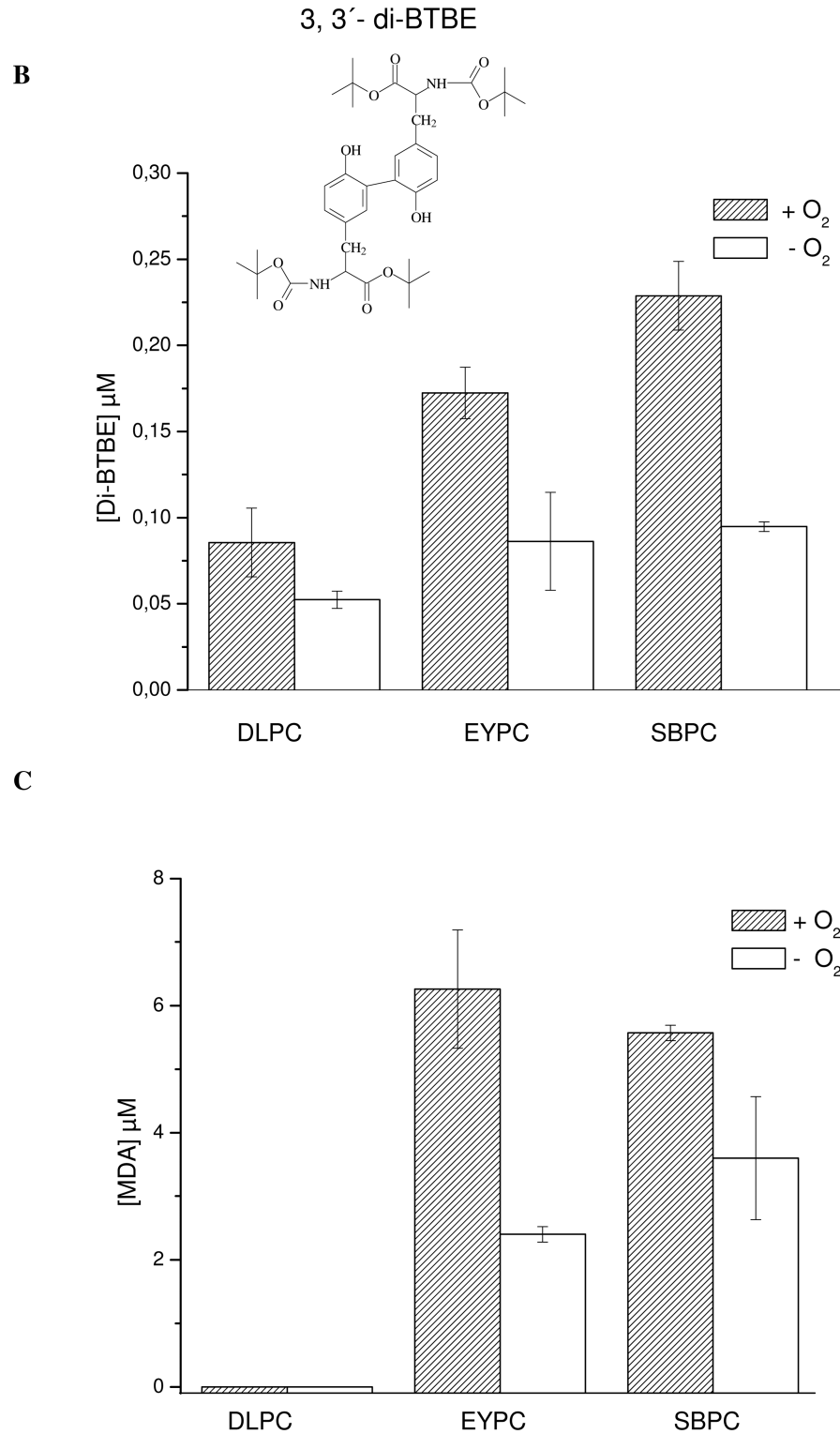


Figure 1. Effect of oxygen on peroxynitrite-dependent BTBE oxidation
 BTBE (0.3 mM) was incorporated to the different liposomes, DLPC, EYPC and SBPC (30 mM) and exposed to peroxynitrite (1 mM) in the presence of oxygen (200 μM) or under low oxygen tensions (~ 5 μM). Samples were analyzed for (A) 3-nitro-BTBE, (B) 3,3'-di-BTBE

and (C) MDA content. Basal MDA levels in EYPC, SBPC and DLPC were 4.88 ± 1.09 ; 4.97 ± 0.72 and 0, respectively. Structures of 3-NO₂- *N-t*-BOC L-tyrosine *tert* butyl ester (3-nitro-BTBE) and 3,3'-di *N-t*-BOC L-tyrosine *tert* butyl ester (3,3'-di-BTBE) are indicated in the corresponding panels.

\$watermark-text

\$watermark-text

\$watermark-text

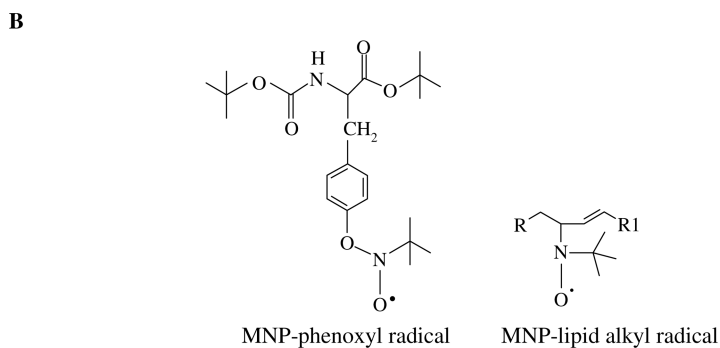
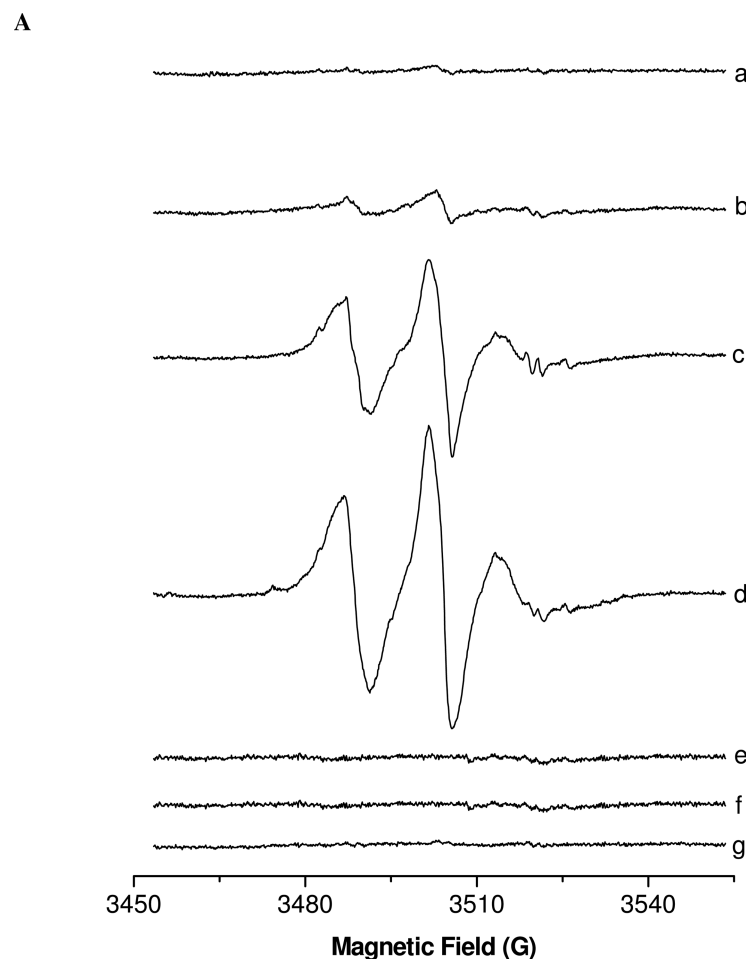


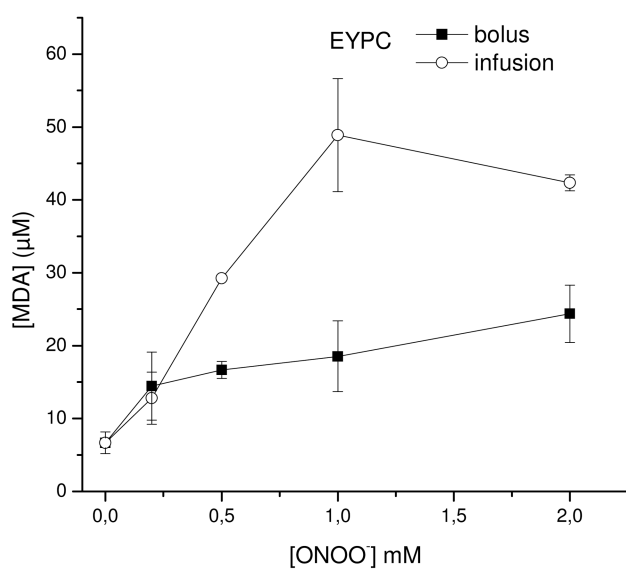
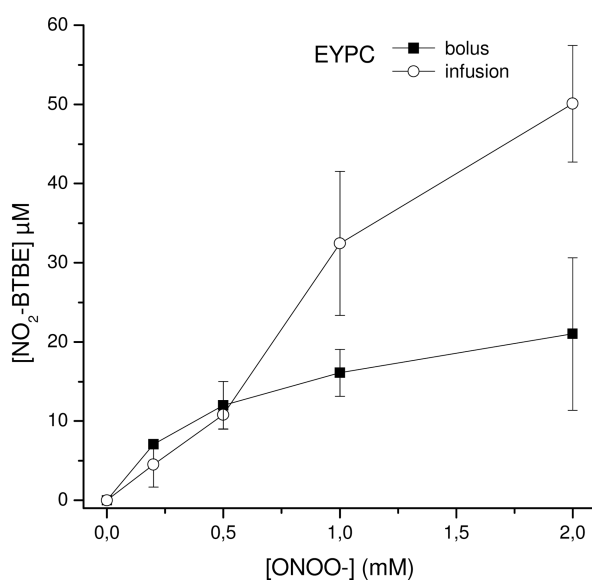
Figure 2. Electron spin resonance- spin trapping of BTBE phenoxy and lipid peroxy radical
(A) Reaction mixtures consisting on BTBE (2.5 mM) incorporated into 45 mM DLPC liposomes in phosphate buffer 100 mM (pH 7.4) containing dtpa (0.1 mM) were treated with 20 mM 2-methyl-2-nitrosopropane (MNP) spin trap and rapidly mixed with 5 mM peroxynitrite. Samples were subsequently transferred to a 50- μ l capillary tube for EPR measurements. (a) DLPC liposomes plus peroxynitrite; (b) BTBE-containing DLPC liposomes plus peroxynitrite; (c) EYPC liposomes plus peroxynitrite; (d) BTBE-containing EYPC liposomes plus peroxynitrite; (e) Same as B with reverse order addition of peroxynitrite; (f) Same as D with reverse order addition of peroxynitrite; (g) Peroxynitrite only. (B) The structures of the MNP-phenoxy and MNP-lipid alkyl radical adducts are

shown and correspond to the signals obtained in lines b and c of panel A, respectively. Both spin adducts are present in line d.

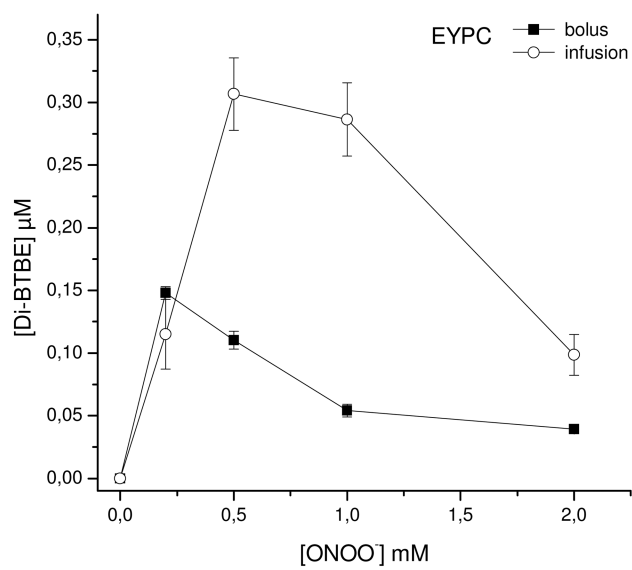
\$watermark-text

\$watermark-text

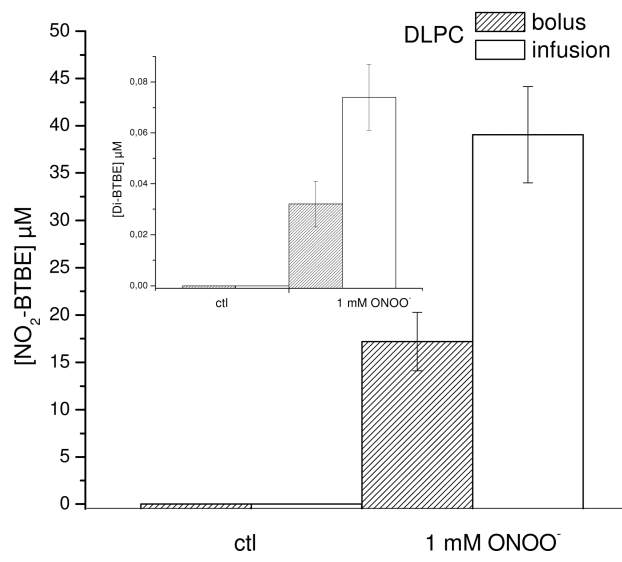
\$watermark-text

A**B**

C



D



E

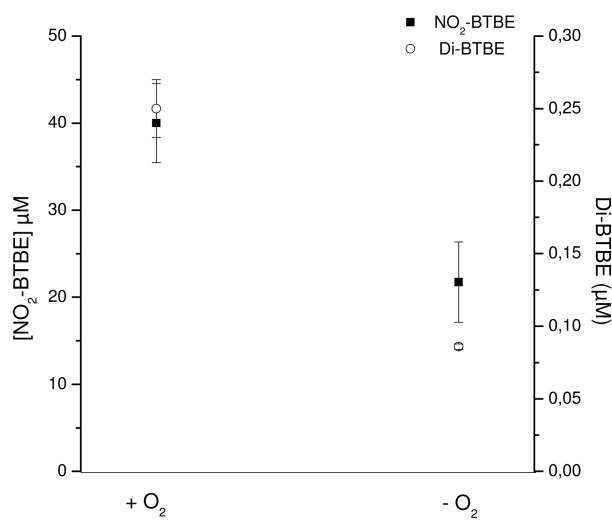


Figure 3. Peroxynitrite-mediated oxidations: slow infusion versus bolus addition
BTBE (0.3 mM) was incorporated to EYPC and DLPC liposomes (30 mM) and exposed to peroxynitrite either as a single bolus (■) or by slow infusion (○) in order to achieve final concentrations of (0.2–2 mM). Samples were analyzed for 3-nitro-BTBE, 3,3'-di-BTBE and MDA content. **EYPC:** (A) MDA (B) 3-nitro-BTBE (C) 3,3'-di-BTBE; **DLPC:** (D) 3-nitro-BTBE and 3,3'-di-BTBE (inset); (E) BTBE (0.3 mM) containing liposomes were exposed to slow infusion of peroxynitrite (1 mM) in the presence and absence of oxygen and 3-nitro-BTBE and 3,3'-di-BTBE was measured as previously.

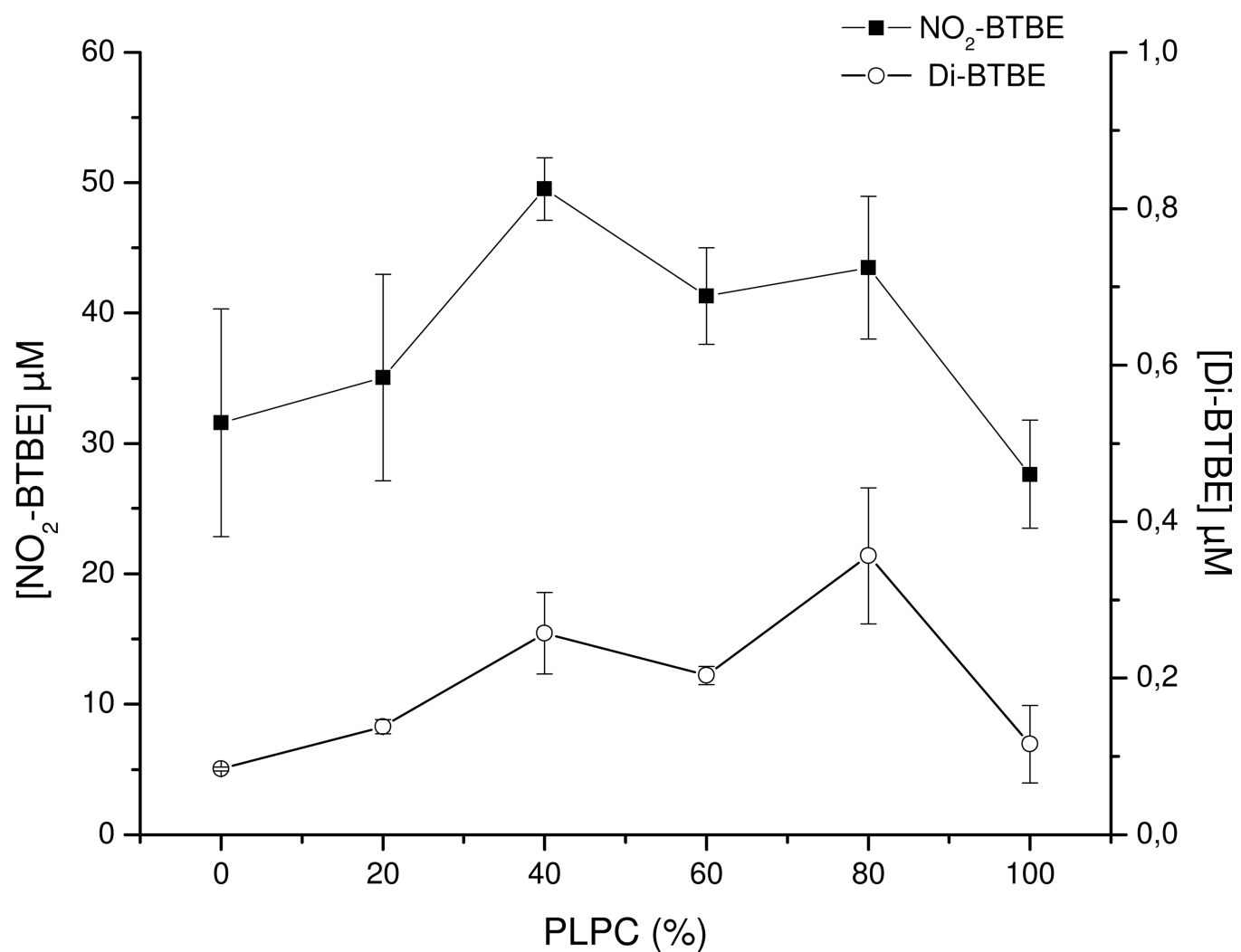


Figure 4. Lipid unsaturation degree and BTBE oxidation

BTBE nitration (■) and dimerization (○) were studied as a function of fatty acid unsaturation by using mixtures of DLPC and PLPC (0–100% PLPC) liposomes containing 0.3 mM of BTBE and treated with peroxynitrite (1 mM).

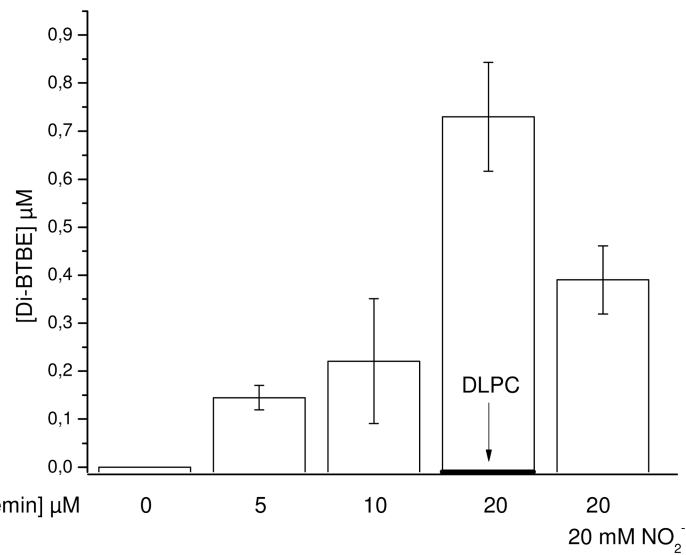
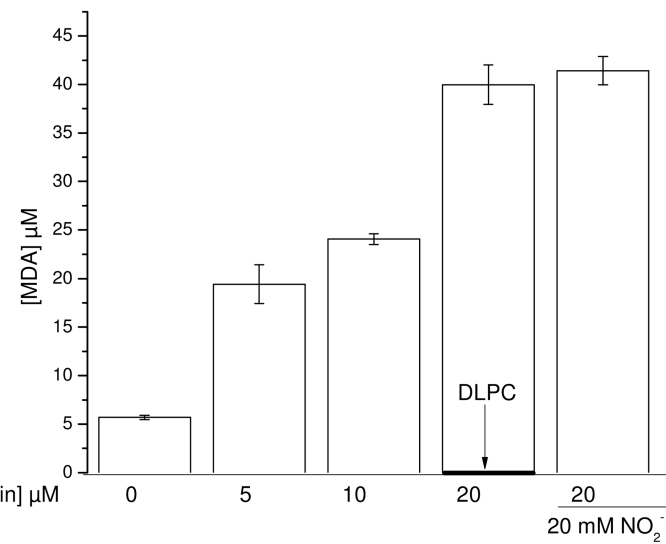
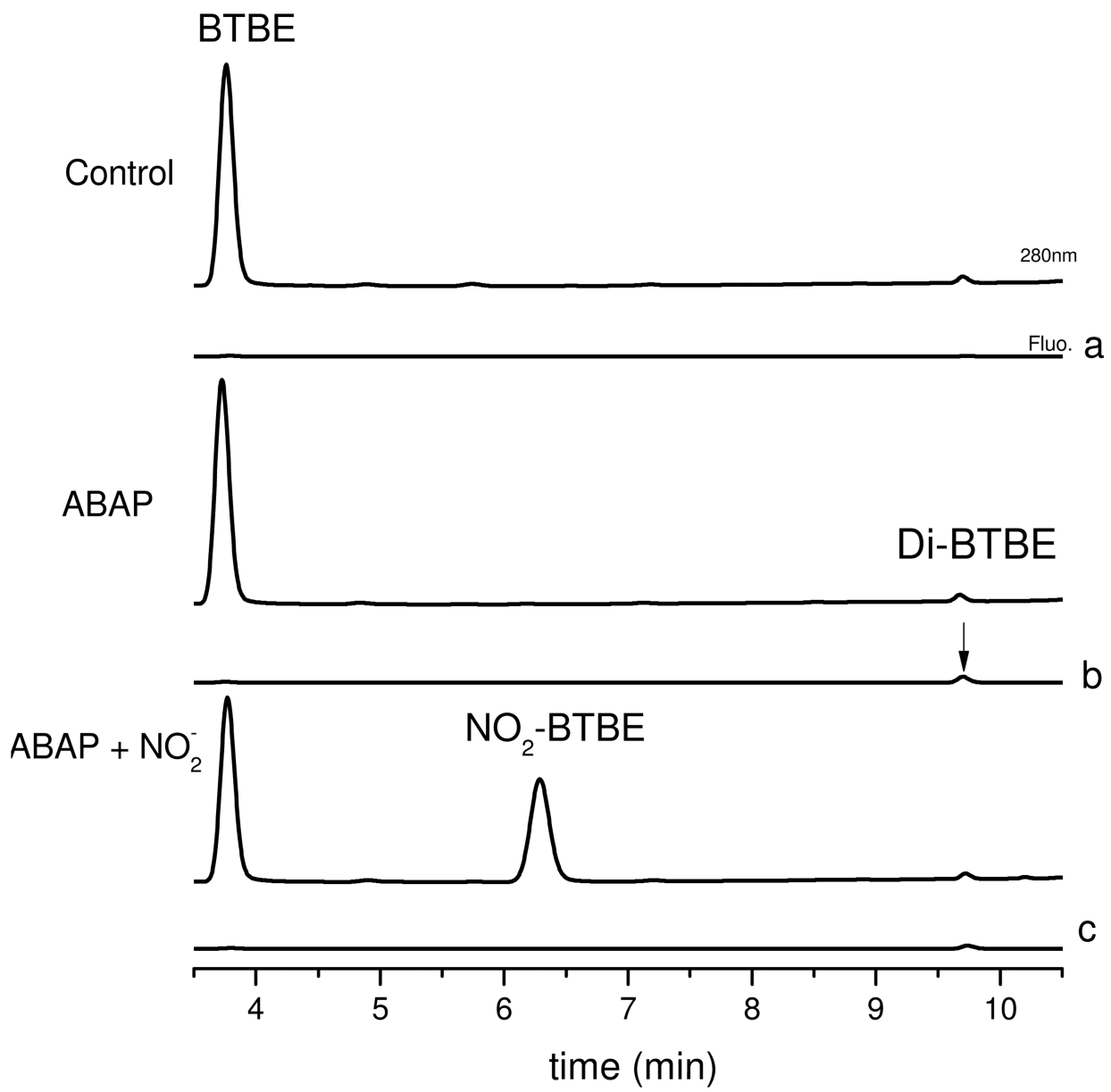
A**B**

Figure 5. Hemin-induced lipid peroxidation and BTBE oxidation

BTBE (0.3 mM)-containing DLPC and EYPC liposomes (30 mM) were exposed to hemin (5–20 μM) in sodium phosphate 100 mM pH 7.3 plus 0.1 mM DTPA. Samples were analyzed for (A) 3,3'-di-BTBE and (B) MDA content. The arrow indicates the values corresponding to DLPC liposomes which were zero for both measurements under all reaction conditions.

A

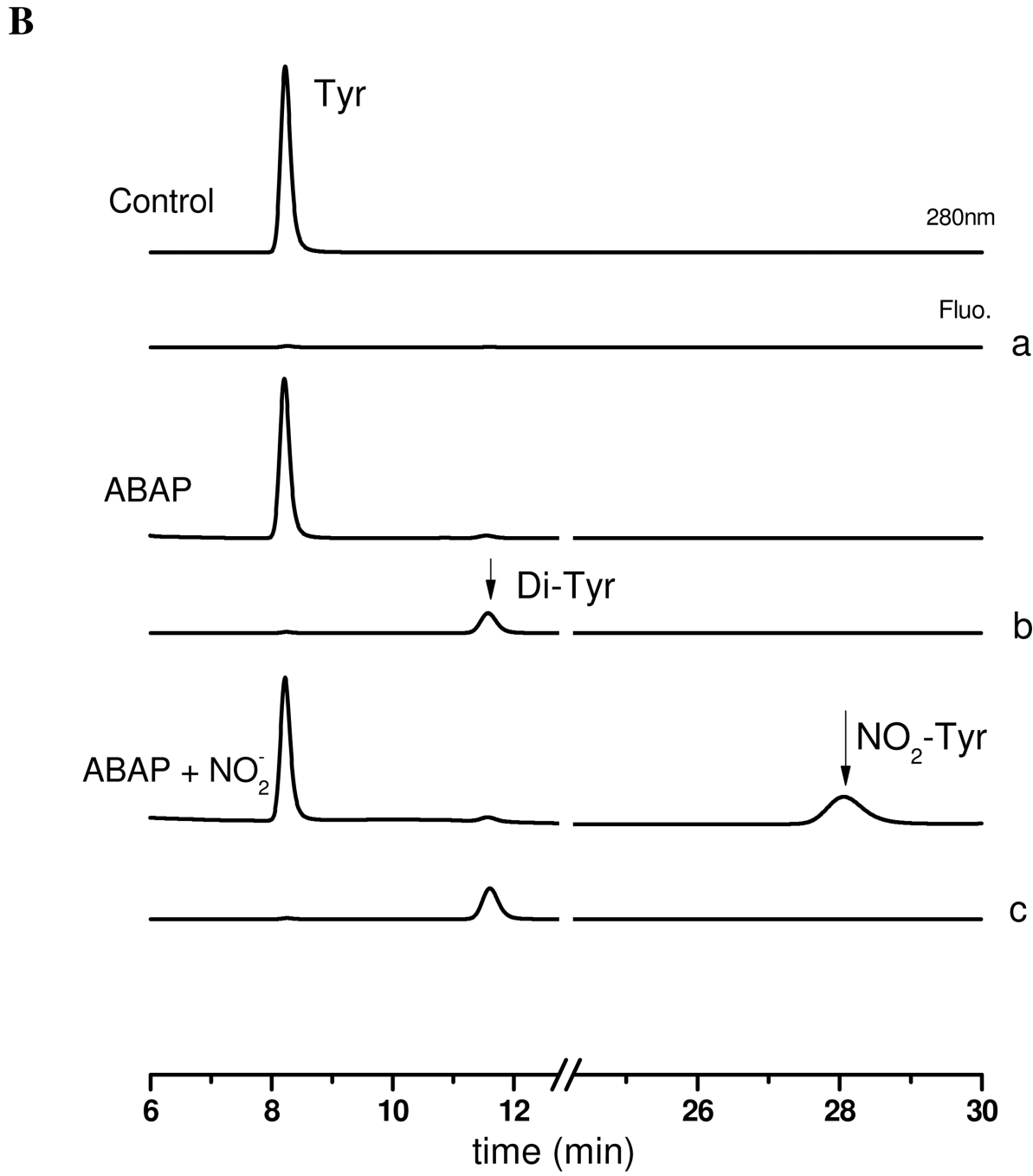


Figure 6. ABAP-induced BTBE and tyrosine oxidation

Panel A: (a) BTBE (0.3 mM)-containing DLPC liposomes in sodium phosphate 100 mM (pH 7.3) plus 0.1 mM DTPA were exposed to (b) ABAP (20 mM) in the absence and (c) presence of nitrite (40 mM) and 3-nitro-BTBE and 3,3'-di-BTBE were measured. **Panel B:** (a) Tyrosine (0.3 mM) in sodium phosphate 100 mM (pH 7.3) plus 0.1 mM DTPA was exposed to (b) ABAP (20 mM) in the absence and (c) presence of nitrite (40 mM) and 3-nitrotyrosine and 3,3'-dityrosine were measured.

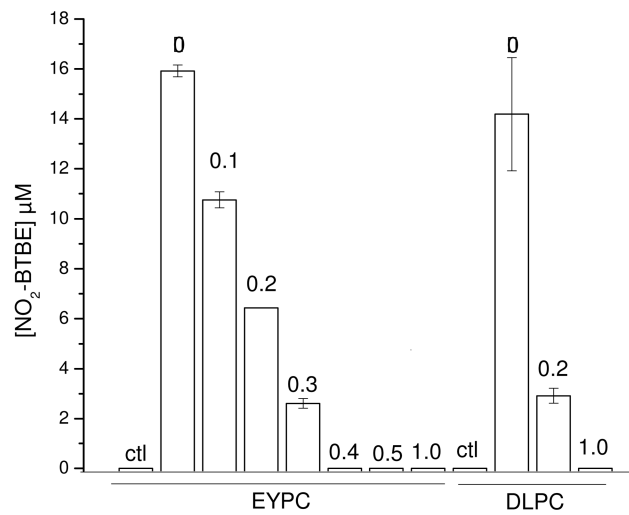
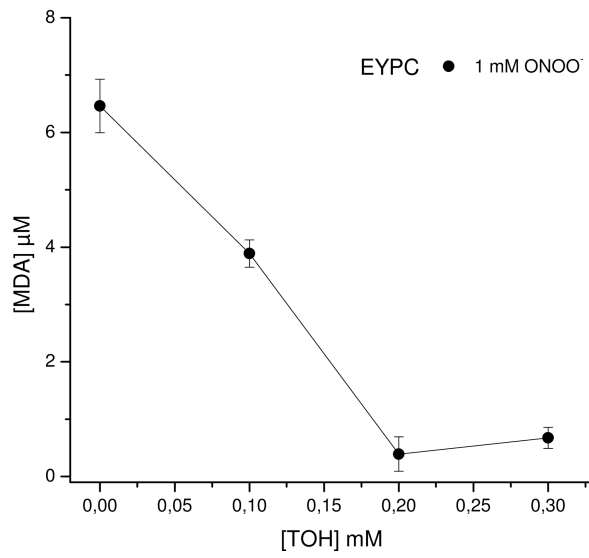
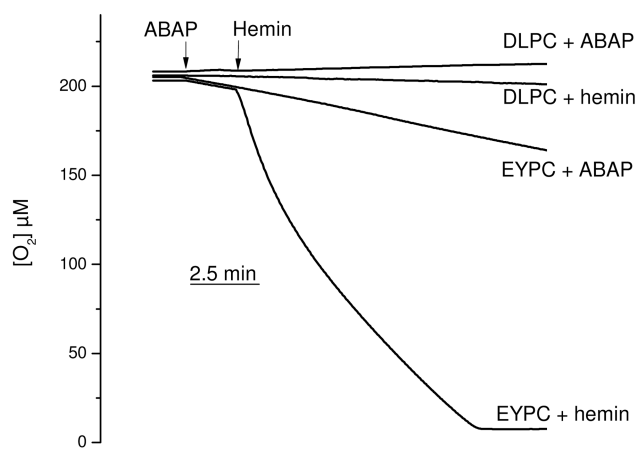
A**B**

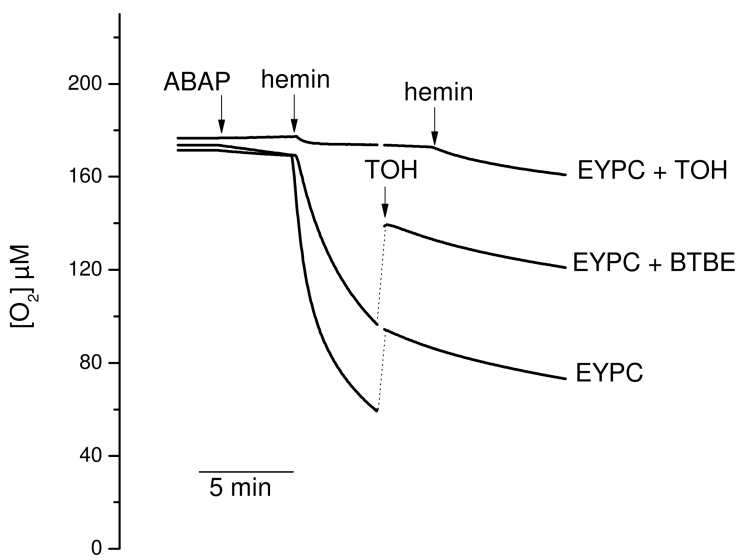
Figure 7. Effect of α -tocopherol on lipid peroxidation and BTBE oxidation

The indicated concentrations of α -tocopherol (0.1–1 mM) were pre-incorporated to different EYPC and DLPC preparations (30 mM) and treated with peroxyynitrite (1 mM); Samples were analyzed for (A) 3-nitro-BTBE and (B) MDA content.

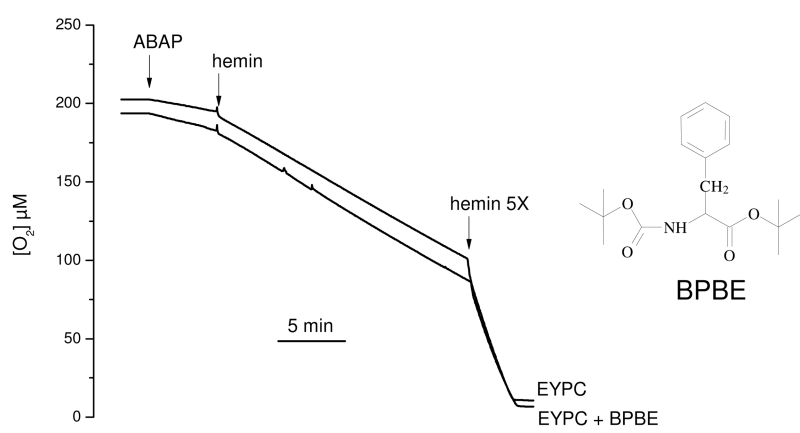
A



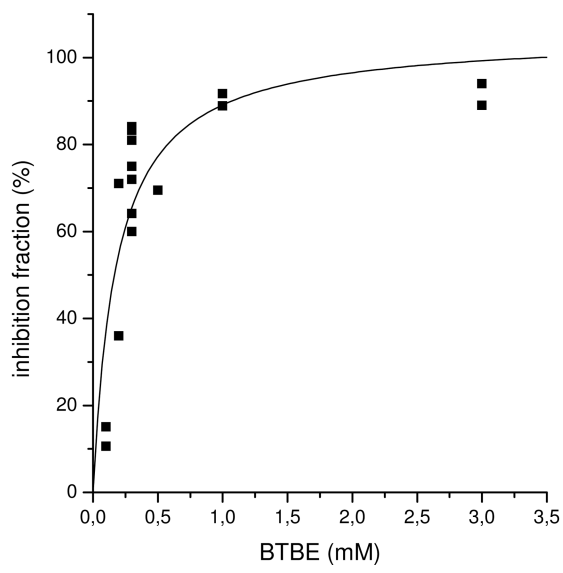
B



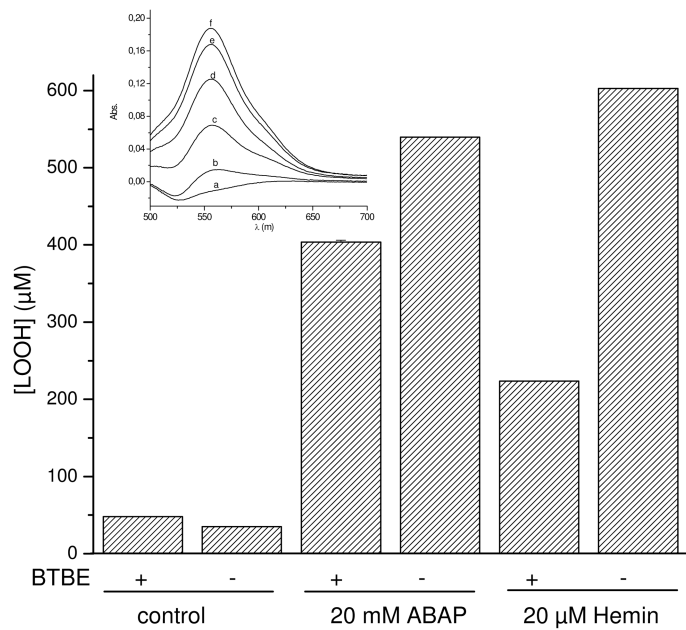
C



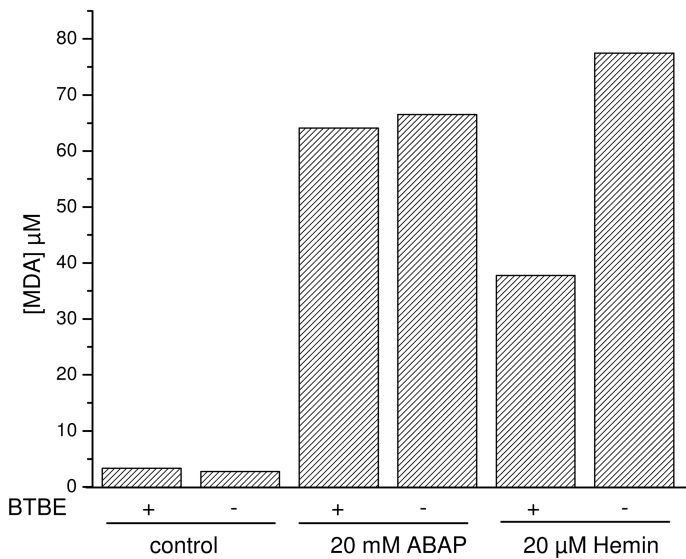
D



E



F

**Figure 8. Oxygen consumption studies**

Oxygen consumption was measured in a 2K Oxygraph to assess ABAP (10 mM) and hemin (1 μM)-induced lipid peroxidation in sodium phosphate 100 mM (pH 7.3) plus 0.1 mM DTPA. (A) EYPC and DLPC liposomes (6.25 mM). (B) BTBE (0.3 mM), or α -tocopherol (0.3 mM) containing EYPC liposomes. The arrow indicates the exogenous addition of 0.25 mM of α -tocopherol; the transient increase in oxygen levels observed in this record is due to oxygen dissolved in the volume of reagent added (C) BPBE (0.3mM) and control EYPC liposomes. (D) EYPC liposomes in the absence and presence of different concentrations of BTBE (0.1 –3 mM) were exposed to ABAP (10 mM) and hemin (1 μM) and oxygen consumption inhibition was evaluated as a function of BTBE concentration. (E) EYPC

liposomes with or without BTBE (0.3 mM) were exposed to hemin (30 min) and ABAP (2.5 h) and lipid hydroperoxide content was measured: Inset: UV-Vis spectra of same samples shown in E (a) – BTBE; (b) + BTBE; (c) + BTBE + hemin; (d) + BTBE + ABAP; (e) – BTBE + ABAP; (f) – BTBE + hemin. (F): Same samples as (E) in which MDA content was measured. The structure of *N-t*-BOC L-phenylalanine *tert* butyl ester (BPBE) is indicated in the corresponding panel.

\$watermark-text

\$watermark-text

\$watermark-text

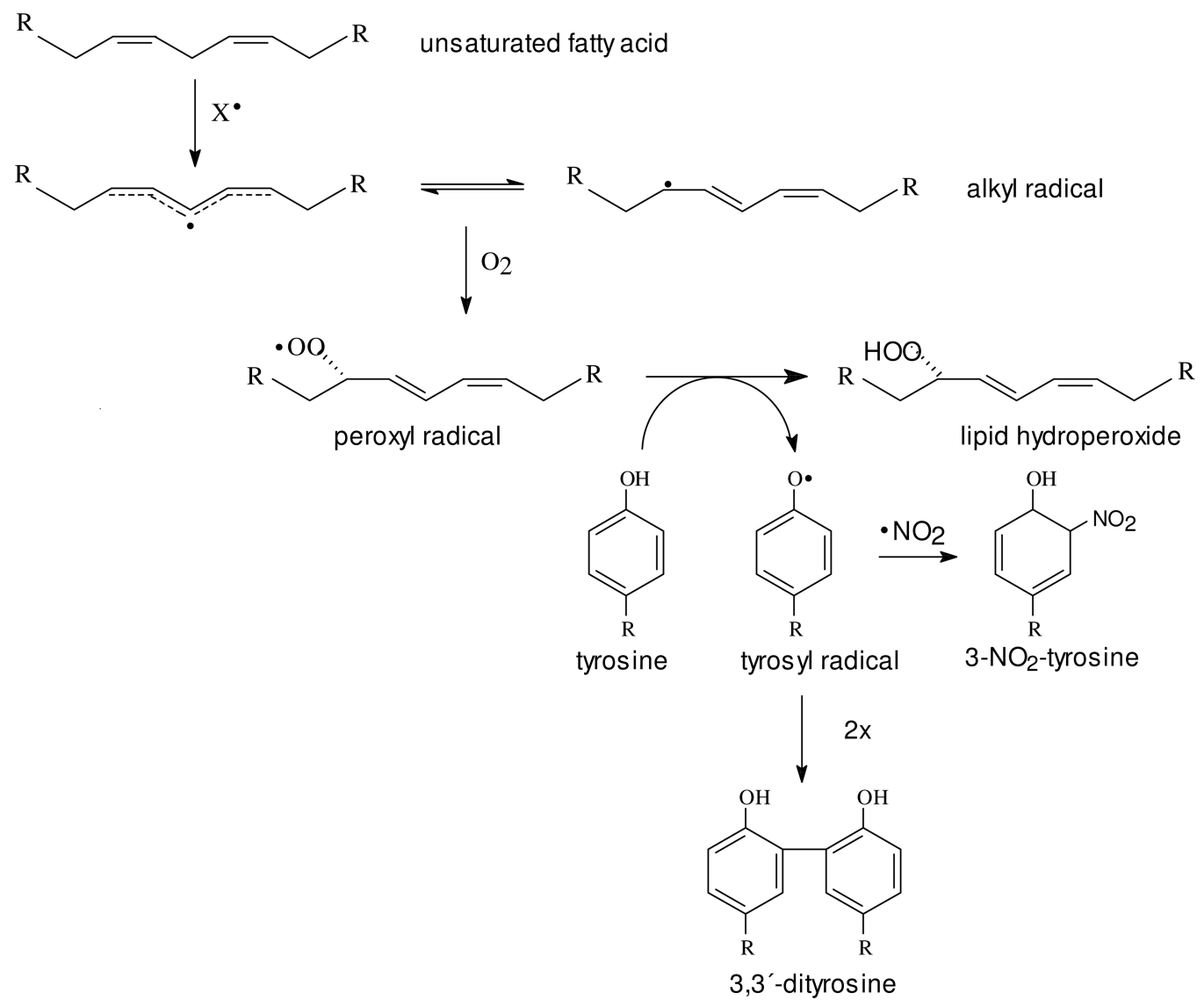
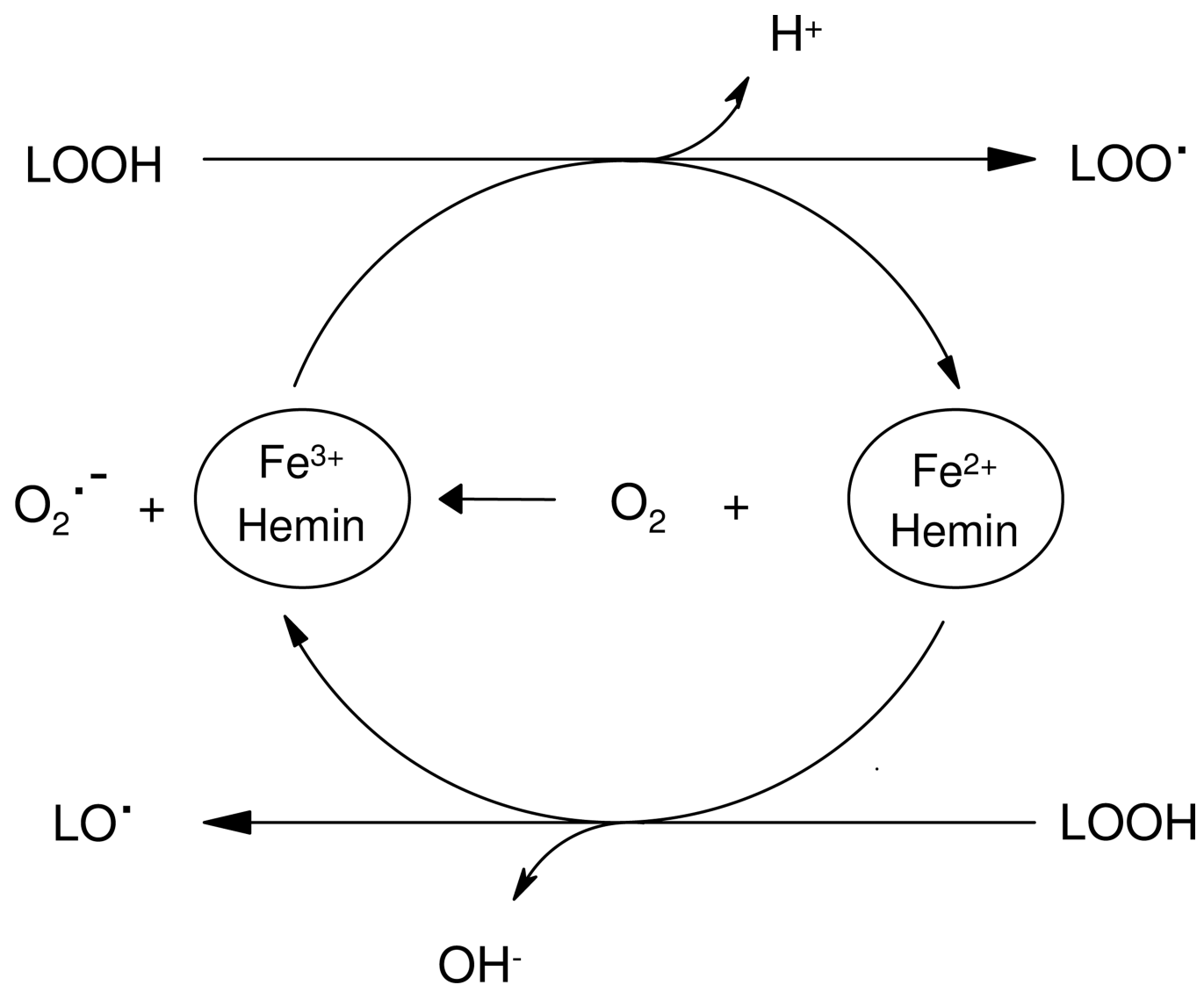


Figure 9. Proposed reaction mechanism by which lipid peroxy radicals participate in tyrosine oxidation



Scheme 1. Lipid hydroperoxide reactions with hemin and lipid-derived radicals formation
Lipid hydroperoxide (LOOH) can react with hemin either in Fe^{3+} or Fe^{2+} redox states to yield LOO^{\bullet} or LO^{\bullet} , respectively. Secondarily, hemin in the reduced state (Fe^{2+}) can yield O_2^- that can further participate in redox reactions.

Table 1
ABAP-mediated BTBE oxidation

BTBE (0.3 mM) was incorporated to DLPC and EYPC liposomes (30 mM) and the mixture incubated during 2h at 37°C with ABAP (10 mM, 0.3 µM /min flux of peroxy radical) in the presence and absence of nitrite (NO_2^-) (20 mM) and 3-nitro-BTBE and 3,3'-di-BTBE content was measured. The same experiment was performed in the presence and low oxygen tension (~ 5 µM).

Condition	EYPC		DLPC	
	$\text{NO}_2\text{-BTBE}$ (µM)	Di-BTBE (µM)	$\text{NO}_2\text{-BTBE}$ (µM)	Di-BTBE (µM)
Control	0	0	0	0
ABAP	0	0.011 ± 0.001	0	0.79 ± 0.164
ABAP + NO_2^-	2.5 ± 0.76	0.043 ± 0.008	16.15 ± 1.39	0.537 ± 0.029
ABAP – O_2	0	0	0	0.32 ± 0.065
ABAP + NO_2^- - O_2	1.46 ± 0.8	ND*	9.43 ± 2	ND
NO_2^-	0	0	0	0

* ND: Not Determined

Table 2
Main reactions involved in tyrosine oxidation in hydrophobic environments and the connection to lipid peroxidation

Reaction	<i>k</i> (M ⁻¹ s ⁻¹)	Reference
^a L + •OH → L• + OH ⁻	1 × 10 ¹⁰	(45)
L + •NO ₂ → L• + NO ₂ ⁻	2 × 10 ⁵	(46)
Tyr + •OH → •Tyr + OH ⁻	1.24 × 10 ¹⁰	(90)
Tyr + •OH → •TyrOH ^b + OH ⁻	6.5 × 10 ⁸	(90)
Tyr + •NO ₂ → •Tyr + NO ₂ ⁻	3.2 × 10 ⁵	(46)
•Tyr + •NO ₂ → 3-nitro-Tyr	3 × 10 ⁹	(46)
2 •Tyr → 3-3'-diTyr	2.25 × 10 ⁸	(91)
	^c 2.25 × 10 ⁶	(41)
L• + O ₂ → LOO•	3 × 10 ⁸	(92)
LOO• + L → LOOH + •L	3 ⁷	(68)
2 LOO• → LOOH + O ₂	10 ⁷	(92)
LOO• + L• → LOOL	5 × 10 ⁷	(92)
2 L• → LL	5 × 10 ⁸	(92)
LOO• + NO ₂ ⁻ → LOOH + •NO ₂	4.5 × 10 ⁶	(65) ^d
LOO• + Tyr → LOOH + •Tyr	4.8 × 10 ³	This work
^e α-Tocopherol + LOO• → α-Tocopheryl• + LOOH	5 × 10 ⁵	(67)
α-Tocopherol + •NO ₂ → α-Tocopheryl• + NO ₂ ⁻	1 × 10 ⁵	(67)
α-Tocopherol + •OH → α-Tocopheryl• + OH ⁻	3.8 × 10 ⁹	(66)

Reactions involving lipids refer to those containing unsaturated fatty acid unless otherwise indicated.

^alipids composed of saturated fatty acid are also oxidized by hydroxyl radicals at similar rates (58).

^bthis radical rapidly dehydrates and evolves to tyrosyl radical under the experimental conditions employed herein.

^cvalue for tyrosine dimerization in membranes, expected to occur at least 100-times slower than in aqueous phase.

^dthis rate constant has been reported for acetylperoxy radical reduction by nitrite.

^ethe radical scavenging mechanisms of α-tocopherol are indicated.